NASA TECHNICAL MEMORANDUM

NASA TM X-53589

October 5, 1967

NASA TM X-53589

SPACE VEHICLE LOW GRAVITY FLUID MECHANICS PROBLEMS AND THE FEASIBILITY OF THEIR EXPERIMENTAL INVESTIGATION

By Gordon K. Platt
Propulsion and Vehicle Engineering Laboratory

NASA

George C. Marshall Space Flight Center, Huntsville, Alabama

GPO PRICE $ _____

CFSTI PRICE(S) $ _____

Hard copy (HC) 3.00

Microfiche (MF) .65

ff 653 July 65

TECHNICAL MEMORANDUM X-53589

SPACE VEHICLE LOW GRAVITY FLUID MECHANICS PROBLEMS AND THE FEASIBILITY OF THEIR EXPERIMENTAL INVESTIGATION

By

Gordon K. Platt

George C. Marshall Space Flight Center

Huntsville, Alabama

ABSTRACT

Liquid motions created within the propellant tanks during vehicle acceleration and persisting into the orbital coast of flight are identified. The magnitudes of the motions are estimated and the capabilities and limitations of various test facilities for their investigation are established. A means of attenuating the liquid motions is suggested.

Several types of tests are considered for the investigation of the phenomena.

Subscale tests may be performed to study initial transient fluid motions induced by several of the phenomena. Since significant damping would not occur during the subscale tests, it is recommended that rocket vehicles be used for tests of sufficient duration to observe the fluid motions until substantial damping has occurred.

NASA-GEORGE C. MARSHALL SPACE FLIGHT CENTER

NASA-GEORGE C. MARSHALL SPACE FLIGHT CENTER

TECHNICAL MEMORANDUM X-53589

SPACE VEHICLE LOW GRAVITY FLUID MECHANICS PROBLEMS AND THE FEASIBILITY OF THEIR EXPERIMENTAL INVESTIGATION

By

Gordon K. Platt

FLUID MECHANICS AND THERMODYNAMICS BRANCH
PROPULSION DIVISION
PROPULSION AND VEHICLE ENGINEERING LABORATORY
RESEARCH AND DEVELOPMENT OPERATIONS

TABLE OF CONTENTS

TABLE OF CONTENTS (Concluded)

LIST OF ILLUSTRATIONS

LIST OF TABLES

DEFINITION OF SYMBOLS

A	Cross sectional area or area contacted, ft^2
a	Acceleration, ft/sec^2
Bo	Bond number, $L^2\rho a/\sigma$
b	Distance liquid projects forward of original interface, ft
C	A constant, $a\beta\dot{q}_w/c_p\nu^3$, ft^{-4}
C_D	Drag coefficient, $F/\rho V^2 A$
c_p	Specific heat at constant pressure, $Btu/lb_m\ °R$
D	Container diameter, ft
E	Energy, $ft\text{-}lb_f$
F	Force, lb_f
Fr	Froude number
$\overline{FS}$	Factor of safety
f	Natural frequency
g_e	Acceleration equal to that due to gravity at the earth's surface, $32.2\ ft/sec^2$
g_o	Conversion factor, $32.2\ lb_m\text{-}ft/lb_f\text{-}sec^2$
h	Height of liquid above tank bottom, ft
h_e	Height of liquid above tank bottom for a flat bottom tank containing the same volume, ft
K	$\tanh 2\alpha\ (h_e/D)$
k	Thermal conductivity, $Btu/ft\ hr\ °R$
L	A characteristic length, ft
m	Mass in general or total mass of liquid in tank, lb_m
p	Tank ullage pressure (absolute), lb_f/in^2
p_o	Tank ullage pressure (gage), lb_f/in^2
$\dot{q}$	Heat flux

R	Tank radius, ft
Re	Reynolds number $VL\rho/\mu$
Ra*	Modified Rayleigh number, $X^4 a\beta\dot{q}_w \rho c_p/\nu k^2$
t	Time or wall thickness, sec or hr or ft
U	Velocity parallel to tank wall in longitudinal direction, ft/sec
u	Eddy velocity, ft/sec
u_1	Characteristic velocity of boundary layer, ft/sec
$\bar{u}$	Mean velocity, ft/sec
V	A velocity, ft/sec
We	Weber number $\rho V^2 L/\sigma$
X	Boundary layer run length, ft
Y	Modulus of elasticity, lb_f/ft^2
y	Distance perpendicular to tank wall, ft
α	The first zero of $J_1'(X)$, 1.84
β	Coefficient of thermal expansion, $°R^{-1}$ Coefficient of isothermal compressibility, ft^2/lb_f
δ	Boundary layer thickness, ft
ζ	Wave amplitude, ft
ζ_s	Maximum (splashing) wave amplitude, ft
λ	Square of the ratio of exciting frequency to first natural frequency
μ	Dynamic viscosity, $lb_m/hr\text{-}ft$
ν	Kinematic viscosity, ft^2/hr
ρ	Density, lb_m/ft^3
σ	Surface tension, lb_f/ft
σ_y	Yield stress, lb_f/in^2
τ	Time for a cycle of motion or time in general, sec

Subscripts

1	Initial condition or environment
2	Second condition or environment
BL	Boundary layer
D	Downward flow

DEFINITION OF SYMBOLS (Concluded)

DR	Draining
h	At the liquid surface
L	Pertaining to the liquid
m	Pertaining to the model
max	Maximum value
p	Pertaining to the prototype
R	Based on tank radius
r	In the radial direction
S	During deceleration (stopping)
T	Pertaining to the tank
w	Pertaining to the tank wall
θ	In the tangential direction
x	In the longitudinal direction

TECHNICAL MEMORANDUM X-53589

SPACE VEHICLE LOW GRAVITY FLUID MECHANICS PROBLEMS AND THE FEASIBILITY OF THEIR EXPERIMENTAL INVESTIGATION

By

Gordon K. Platt
George C. Marshall Space Flight Center
Huntsville, Alabama

SUMMARY

It was the purpose of this study to identify sources and define magnitudes of propellant motions that may disturb the liquid-vapor interface and interfere with space vehicle propellant tank venting after insertion into orbital coast, examine the possibility of experimentally investigating them in subscale tests, and determine whether long duration (orbital) experiments are needed.

From the analyses described in this text, it was concluded that propellant sloshing and thermal convection induced during space vehicle boost flight, and the release of tank-wall and liquid-stored strain energy at insertion into orbit, are the sources of propellant motion that will present problems in orienting liquid within propellant tanks during orbital coast. To attenuate these motions, it is suggested that conventional ring-type baffles be placed within the tank.

The initial fluid motions resulting from induced sloshing and from liquid-stored strain energy can be investigated in drop tower tests. A complete investigation of liquid motion in orbital coast resulting from any of the phenomena identified will require an orbital experiment.

I. INTRODUCTION

To accomplish certain space flight missions, including the lunar landing, it will be advantageous to allow the vehicle to coast in earth orbit for a time before the terminal stage of the launch vehicle makes its final engine burn and accelerates to earth escape velocity (Ref. 1). Vehicles using cryogenic propellants will generally require venting during the orbital coast to avoid an excessive rise of tank pressure. Propellant motions induced during engine burning or at injection into orbit are expected to persist for extended periods during orbital coast. While gravitational forces will not be absent, the statics or dynamics of a system relative to the vehicle may be treated as if it were in a very low gravity field. Thus, the forces available to separate liquid from vapor for propellant tank venting will be very small. Chaotic motions may well be created within the tank, and excessive venting of liquid may be unavoidable.

Much study has been devoted to determining equilibrium liquid-vapor interface shapes during the absence, or near absence, of gravity forces, but little study has been devoted to determining whether propellant motions can be expected and their duration and effect on liquid location. Also, no comprehensive study has been made to determine how such motions may be experimentally investigated.

It is the purpose of this study to (1) identify the sources and define the magnitudes of propellant motions that may disturb the liquid-vapor interface and interfere with space vehicle propellant tank venting after insertion into orbital coast, (2) examine the possibility of experimentally investigating them in subscale tests, and (3) determine whether long duration (orbital) experiments are needed.

II. REVIEW OF PREVIOUS WORK

Until very recently, efforts in zero and low gravity fluid mechanics were concerned almost exclusively with static equilibrium configurations of liquid-vapor interfaces in containers of simple shape. Li (Ref. 2) and Benedikt (Ref. 3) performed much of this work. Experimental data on low gravity boiling heat transfer in liquid nitrogen were obtained by Merte and Clark (Ref. 4) and in liquid hydrogen by Clodfelter (Ref. 5). Otto, et al. (for example, see Ref. 6) published several papers concerning experimental determination of liquid-vapor interface shapes in quiescent fluids in zero gravity, and concerning the time for deformation of the liquid-vapor interface from its shape in a one earth gravity (1 ge) field to its shape in zero gravity. Chin, et al. (Ref. 7) did further work on the equilibrium liquid-vapor interface shape in cylindrical containers in low gravity and extended their results to account for modifications of the interface shape by convection induced by axisymmetric heating. Reynolds (Ref. 8) presented a comprehensive discussion of basic zero and low gravity hydrodynamics in a report that was used extensively as a basis for parts of this study. He also presented the first analysis known to the author that indicated the propellant configuration in space vehicle tanks in earth orbit would be dominated by acceleration-induced body forces. Gluck and Gille (Ref. 9) and Bowman (Ref. 10) recently published analytical and experimental studies of the initial motion of propellant reorientation in low gravity. Gluck and Gille also presented a cursory discussion of other sources of propellant motion in low gravity. Satterlee and Reynolds (Ref. 11) recently published experimental results and an analytical treatment of small amplitude sloshing in low gravity.

The emphasis on hydrostatics in zero and low gravity, evidenced by the great deal of attention this area has received, has been well placed. Any study of low gravity fluid location and motion in containers must begin with a knowledge of the equilibrium configuration. Until quite recently, however, the tendency was to ignore the sources of fluid motion and assume a static situation (Refs. 2, 3, and 6).

An awareness of some of the sources of fluid motion in space vehicle tanks is evidenced by the more recent work of References 7, 9, 10, and 11. While this latter work is useful, and Reference 9 presents the framework of a thorough study of all sources of propellant motion in "storable" propellants in low gravity, no comprehensive study has been published that treats all the identifiable sources of propellant motion. Further, while References 4 and 5 are valuable as basic data concerning heat transfer to cryogenic fluids in low gravity, only Reference 7 treats the resulting liquid motions. This work, however, was confined to the study of thermally induced convective patterns in containers being steadily accelerated at a low acceleration. Unfortunately, no study has been made to define the fluid motions set up during a high acceleration but persisting after the acceleration of the container has been reduced.

III. ANALYSIS OF THE SOURCES OF PROPELLANT MOTION

The phenomena that cause propellant motion during acceleration of a space vehicle are: sloshing induced during powered flight, thermally induced propellant motion, tank draining, and strain energy stored in the propellant and propellant tank structure. The general theory of each phenomenon is considered separately below.

A. Sloshing Induced During Powered Flight

One of the major potential sources of momentum in the liquid propellant of a space vehicle at insertion into orbit is sloshing formed during powered flight. A space vehicle is subjected to wind forces and makes various maneuvers to follow its programmed trajectory. Thus, lateral disturbances of the vehicle are introduced. When a container of liquid is subjected to lateral disturbances, the liquid sloshes. Sloshing is the oscillatory motion of the essentially planar liquid-vapor interface. The slosh wave energy alternates between kinetic energy (when the wave amplitude is a minimum) and potential energy (when the amplitude is a maximum). The maximum amplitude generally occurs at the container wall; the amplitude is limited, as splashing occurs when the frequency of the lateral excitation of the container approaches the natural frequency of the slosh wave.

The first natural frequency of a body force and surface tension restored slosh wave is given by Reference 9 as:

$$f_1 = \frac{1}{2\pi}\left[\left(\frac{2\alpha}{D}\right)\left(\frac{a_1}{g_e}\right) g_e \tanh\left(\frac{2\alpha h_e}{D}\right) + \left(\frac{2\alpha}{D}\right)^3 \frac{\sigma}{\rho} \tanh\left(\frac{2\alpha h_e}{D}\right)\right]^{1/2} \qquad (1)$$

where:

f_1 = first natural frequency of the wave, sec^{-1}

α = the zeros of $J_1'(X)$ (1.84, the first, applies to the first mode slosh wave)

D = tank diameter, ft

a_1 = acceleration, ft/sec^2

g_e = acceleration of gravity at the earth's surface, ft/sec^2

σ = surface tension, lb_f/ft

ρ = density of liquid, lb_m/ft^3

The first term in the brackets of Eq. (1) represents the contribution due to body force (usually gravity or the inertial reaction to a longitudinal acceleration). The second term accounts for the effect of surface tension. Surface tension may act as either a restoring or a disturbing force since the direction of the surface tension force depends upon the contact angle the liquid surface makes with the tank wall. Equation (1) is strictly true only for a liquid that makes a 90° contact angle with the tank wall. It is true within 8% for a 30° contact angle for $10 \leq Bo \leq 40$ with a decreasing error as Bo increases (Ref. 11). No research exists to define this effect for combinations of liquids and tank materials that result in contact angles less than 30°. Liquid hydrogen and liquid oxygen have contact angles, with all known solids, not measurably different from zero.

Rearranging Eq. (1) and defining the Bond number, $Bo_R = R^2 \rho a/\sigma$, where R = tank radius (ft)

$$f_1 = \frac{1}{2\pi}\left[\frac{a_1}{g_e} g_e \tanh\left(\frac{2\alpha h_e}{D}\right)\left(\frac{2\alpha}{D}\right)\right]^{1/2}\left[1 + \frac{\alpha^2}{Bo_R}\right]^{1/2} \qquad (2)$$

The Bond number represents the ratio of body to surface tension (capillary) forces. It is seen that for the first mode slosh wave and for values of Bo exceeding 34 the second term may be neglected with an error of less than 10%.

Equation (1) will be used herein since it is the best available, even though it is somewhat in error for certain fluids.

If the tank has a fill height that is approximately as great as, or greater than, the tank diameter, $\tanh 2\alpha h_e/D \approx 1$. If Bo is also large, Eq. (2) becomes:

$$f_1 = \frac{1}{2\pi}\left[\left(\frac{2\alpha}{D}\right)\left(\frac{a_1}{g_e}\right) g_e\right]^{1/2} \qquad (3)$$

The maximum amplitude (at which splashing occurs) is given by Eulitz (Ref. 12) as:

$$\zeta_s = \frac{1}{2\alpha\lambda} \frac{D}{K} \tag{4}$$

where:

$$K = \tanh \alpha \frac{h_e}{D} \tag{5}$$

ζ_s = slosh wave amplitude at splashing, ft

α = the first zero of $J_1'(X)$ (1.84)

λ = square of the ratio of exciting frequency to first natural frequency

D = tank diameter, ft

h_e = equivalent liquid level in tank, ft

The total energy of a gravity restored slosh wave, neglecting surface energy and considering the first mode (Ref. 9) is:

$$E_s = 0.553 \rho \frac{a_1}{g_e} R^2 \zeta^2 \tag{6}$$

where:

E_s = wave energy, $ft\text{-}lb_f$

ρ = liquid density, lb_m/ft^3

a_1 = longitudinal acceleration of container, ft/sec^2

R = tank radius, ft

ζ = slosh wave amplitude, ft

The surface energy due to sloshing may be calculated quite simply by multiplying the surface tension of the liquid by the difference between the surface area with and without sloshing (Ref. 8). The wave is planar; thus, in a cylindrical container, the surface is elliptical. The surface energy due to sloshing is:

$$E_{sT} = \pi R^2 \sigma \left[\sqrt{1 + (\zeta/R)^2} - 1\right] \tag{7}$$

B. Thermally Induced Propellant Motion

Prior to launching and during flight through the earth's atmosphere, environmental heating will establish convective motions within the cryogenic propellant of a space vehicle stage. Before insertion into orbit, the warm fluid will rise adjacent to the container walls, due to buoyancy, and spread across the liquid surface. However, when the acceleration is suddenly reduced at insertion, the low acceleration of the vehicle may allow the liquid to continue forward.

By assuming that the liquid motion near the container wall can be described as a boundary layer, successful correlations of observed axial temperature gradients in space vehicle tanks have been made (Ref. 13). A similar approach will be taken here to estimate the mass and velocity of the flowing fluid.

The boundary layer formed on the container walls depends upon the acceleration and history of heat input (or wall temperature). An average heat flux of 0.08 Btu/sec-ft^2 will be assumed (References 13 and 14). This appears to be in the region of the threshold of nucleate boiling, but data are inadequate to confirm this (Ref. 15). Reference 14 assumed an average acceleration of 1.0 ge for stratification analysis of a space vehicle stage. From References 13 and 14, the boundary layer will be almost entirely turbulent (the modified Rayleigh number, Ra* is greater than 10^{11}). From Reference 13, for a turbulent boundary layer, a velocity profile may be assumed of the form:

$$\frac{u}{u_1} = \left(\frac{y}{\delta}\right)^{1/7} \left(1 - \frac{y}{\delta}\right)^4 \tag{8}$$

where:

u = velocity parallel to container wall, ft/sec

u_1 = characteristic velocity of the boundary layer, ft/sec

y = distance perpendicular to container wall, ft

δ = boundary layer thickness, ft

Reference 13 also gives the following expressions for the characteristic velocity and boundary layer thickness:

$$u_1 = 3.72\,\nu\left[\frac{a\beta\dot{q}_w}{\rho c_p \nu^3}\right]^{5/14} X^{3/7} = 3.72\,\nu C^{5/14} X^{3/7} \tag{9}$$

$$\delta = 0.526\left[\frac{a\beta\dot{q}_w}{\rho c_p \nu^3}\right]^{-1/14} X^{5/7} = 0.526\, C^{-1/14} X^{5/7} \tag{10}$$

where:

ν = kinematic viscosity, ft^2/hr

a = vehicle acceleration, ft/sec^2

β = coefficient of thermal expansion, R^{-1}

$\dot{q}_w$ = heat flux to liquid, $Btu/hr\text{-}ft^2$

ρ = liquid density, lbm/ft^3

c_p = specific heat at constant pressure, Btu/lbm-R

X = boundary layer run length, ft

$C = a\beta\dot{q}_w/\rho c_p \nu^3$, a constant, ft^{-4}

The mean velocity across the boundary layer, $\bar{u}y$, is:

$$\bar{u}y = \frac{\int_{y=0}^{\delta} u\,dy}{\int_{y=0}^{\delta} dy} = \frac{\int_0^1 u\,d\left(\frac{y}{\delta}\right)}{\int_0^1 d\left(\frac{y}{\delta}\right)} \tag{11}$$

substituting Eqs. (8) and (9) into Eq. (11) and performing the indicated integration:

$$\bar{u}y = 0.546\,\nu\, C^{5/14} X^{3/7} \tag{12}$$

Assuming axisymmetry and that the boundary layer thickness is small compared to the tank radius, the kinetic energy in the boundary layer may be calculated as follows

$$E_{BL} = \frac{mV^2}{2g_o} = \frac{1}{2g_o}\int_o^h \pi D\delta\rho\,\bar{u}y^2\,dX \tag{13}$$

Substituting Eqs. (10) and (12) into Eq. (13) and integrating:

$$E_{BL} = \frac{0.061\,\pi D \rho v^2 C^{9/14} h^{18/7}}{2g_o} \tag{14}$$

where:

m = mass of liquid participating, lb_m

E_{BL} = kinetic energy in the boundary layer, ft-lbf

V = a velocity of liquid, ft/sec

D = tank diameter

g_o = conversion factor, lbm-ft/lbf-sec^2

h = height of liquid above tank bottom

The other symbols were defined earlier.

The total mass in the boundary layer may be calculated from:

$$m_{BL} = \pi D \rho \int_o^h \delta \, dX \tag{15}$$

Substituting Eq. (10) into Eq. (15) and integrating:

$$m_{BL} = 0.307\,\pi D \rho C^{-1/14} h^{12/7} \tag{16}$$

where m_{BL} is the mass of liquid in the boundary layer and the other symbols are the same as before. Since there is boundary layer flow up the tank walls, continuity dictates that the fluid core move downward. Neglecting draining and assuming an equivalent cylindrical container, a mean velocity of the downward flow, $\bar{u}_D$ may be found. Neglecting density variation in the liquid, the net vertical volumetric flow rate across any plane perpendicular to the tank axis must be zero.

$$\bar{u}_y A_{BL} = \bar{u}_D (A_T - A_{BL}) \tag{17}$$

where:

A_T = cross sectional area of tank, ft^2

A_{BL} = cross sectional area of boundary layer, ft^2

or, if $R \gg \delta$

$$\pi D \delta \bar{u}_y = \bar{u}_D \left[\frac{\pi D^2}{4} - \pi D \delta \right] \tag{18}$$

Substituting Eqs. (10) and (11) into Eq. (18) and solving for $\bar{u}_D$:

$$\bar{u}_D = \frac{1.15 \nu C^{4/14} X^{8/7}}{D - 2.105 C^{-1/14} X^{5/7}} \tag{19}$$

An expression for the kinetic energy of the downward core flow may next be found. The downward-flowing mass at any station X is:

$$dm = \left(\frac{\pi D^2}{4} - \pi D \delta \right) \rho \, dX \tag{20}$$

This mass has a mean velocity of u_D from Eq. (19).

For any element,

$$dE_D = \frac{\bar{u}_D^2 \, dm}{2 g_o} \tag{21}$$

Substituting Eqs. (10), (19) and (20) into Eq. (21),

$$E_D = \frac{\pi D \rho}{8 g_o} \int_o^h \frac{1.15^2 \nu C^{4/7} X^{16/7} dX}{D - 2.105 C^{-1/14} X^{5/7}} \tag{22a}$$

Attempts to integrate Eq. (22a) directly failed, thus this equation was put into the finite difference form:

$$E_D = \frac{\pi D \rho}{8 g_o} [1.15^2 \nu^2 C^{4/7}] \sum_{i=1}^{h/\Delta x} \frac{X^{16/7} \Delta X_i}{[D - 2.105 C^{-1/14} X^{5/7}]} \tag{22b}$$

C. Release of Stored Strain Energy

During the engine burn period, the space vehicle propellant tank sidewalls and lower bulkhead will be deflected and the propellant compressed by the hydrostatic pressures of the propellant within the tank. When the engine is cut off, this

hydrostatic pressure will suddenly be relieved and the tank walls and bulkhead will return, probably in the form of an oscillatory motion, to their undeflected configuration. Also, the liquid will expand to a certain extent.

In Reference 16, the following expression is derived for wall strain energy released by a reduction in acceleration:

$$E_w = \frac{\pi R^3 \rho}{Yt}\left[\frac{\rho h^3}{3}\left(\frac{a_2^2 - a_1^2}{g_o^2}\right) + p_o h^2\left(\frac{a_2 - a_1}{g_o}\right)\right] \qquad (23)$$

where:

E_w = strain energy in cylindrical tank wall, ft-lb_f

Y = elasticity of tank wall material, lb_f/ft^2

t = tank wall thickness, ft

p_o = tank ullage pressure (gage), lb_f/ft^2

The other symbols are the same as defined earlier. To derive this equation it was assumed that the local tank wall stress and deflection in the tangential direction can be computed by the simple hoop stress formula. Also, no account was taken of the energy absorbed by the structure of the tank wall.

Reference 16 also presents an equation for the energy stored within the liquid due to the local hydrostatic pressure that is relieved by a reduction in acceleration:

$$E_L = \frac{\pi R^2 \beta \rho h^2 (a_2 - a_1)}{2g_o}\left[p + \frac{(a_2 + a_1)\rho h}{3g_o}\right] \qquad (24)$$

where:

E_L = strain energy stored in liquid, ft-lb_f

β = coefficient of isothermal compressibility of liquid, ft^2/lb_f

p = tank ullage pressure (absolute), lb_f/ft^2

This equation was derived for a container of uniform **cross** section with a flat bottom.

D. Fluid Motion

The kinetic energy due to tank draining is:

$$E_{DR} = \frac{\rho}{g_o} \int_o^h \int_o^{\pi} \int_o^R (V_r^2 + V_\theta^2 + V_x^2)\, r\, dr\, d\theta\, dx \qquad (25)$$

where:

E_{DR} = kinetic energy of liquid due to draining, ft-lb_f

r = distance from tank center line, ft

θ = angle from a plane passing through the feedline entrance and containing the tank center line, rad

x = distance from the tank bottom, ft

V_i = liquid velocity in the i direction, ft/sec

IV. ANALYSIS OF LIQUID MOTION IN LOW GRAVITY

A space vehicle in earth orbit or coasting in space is not in a gravity free environment. As used in this study, the term "zero gravity" refers to a situation wherein a space vehicle and the liquids within its propellant tanks are subjected to the same acceleration and are in free fall. Thus, the liquids in the tanks behave as if the vehicle were in a gravity free environment and only the forces on the vehicle (other than gravity) need be considered in analyzing propellant behavior (Ref. 10). Without external forces, the propellant location in zero gravity would be governed by surface tension (Refs. 2 and 3).

Reference 8 describes the Bond number as the dimensionless parameter that describes the ratio of body (or acceleration) forces to capillary (surface tension) forces. The Bond number is:

$$Bo = L^2 \rho a / \sigma \tag{26}$$

where:

L = characteristic length of container, ft

ρ = density of liquid, lb_m/ft^3

a = acceleration of container due to external forces, ft/sec^2

σ = surface tension of liquid, lb_f/ft

For a Bond number substantially greater than unity, the quiescent fluid configuration within a container is dominated by the body or acceleration force (Ref. 8).

The Weber number is:

$$We = \rho V^2 L / \sigma \tag{27}$$

where V is the velocity of the liquid and the other symbols are the same as before. The Weber number is the ratio of inertial to capillary forces. For a Weber number

substantially greater than one, inertial forces are considered to be dominant with respect to capillary forces.

The Froude number,

$$Fr = We/Bo = V/\sqrt{aL} \tag{28}$$

is the ratio of inertial forces to body forces.

The Reynolds number,

$$Re = VL\rho/\mu \tag{29}$$

is the ratio of inertial to viscous forces.

Reynolds divides the regimes of hydrodynamic behavior of a fluid as shown in Figure 1. He considers that uncertainty as to regime exists in the areas extending roughly an order of magnitude to either side of the line where any one of these dimensionless numbers equals unity. Reynolds provides no similar guide to the separation of inertial and viscous regimes as characterized by the Reynolds number. Certainly, the transition value of Reynolds number depends strongly on the characteristic length used.

It would be erroneous to assume that the Bond number for space vehicle propellants during orbital coast will always be zero or substantially less than unity. Reference 17 quotes the following magnitudes of acceleration as representative for a space vehicle in a 100 nautical mile earth orbit (with the vehicle orientation maintained perpendicular to the local vertical).

TABLE 1

SUMMARY OF IMPORTANT ACCELERATIONS

Source	Magnitude (ge)
Aerodynamic drag	10^{-6}
Gravity gradient	10^{-6}
Solar Pressure	10^{-9}
Centripetal force	
Rotation about vehicle center of mass	10^{-7}
Attitude control system	10^{-6}

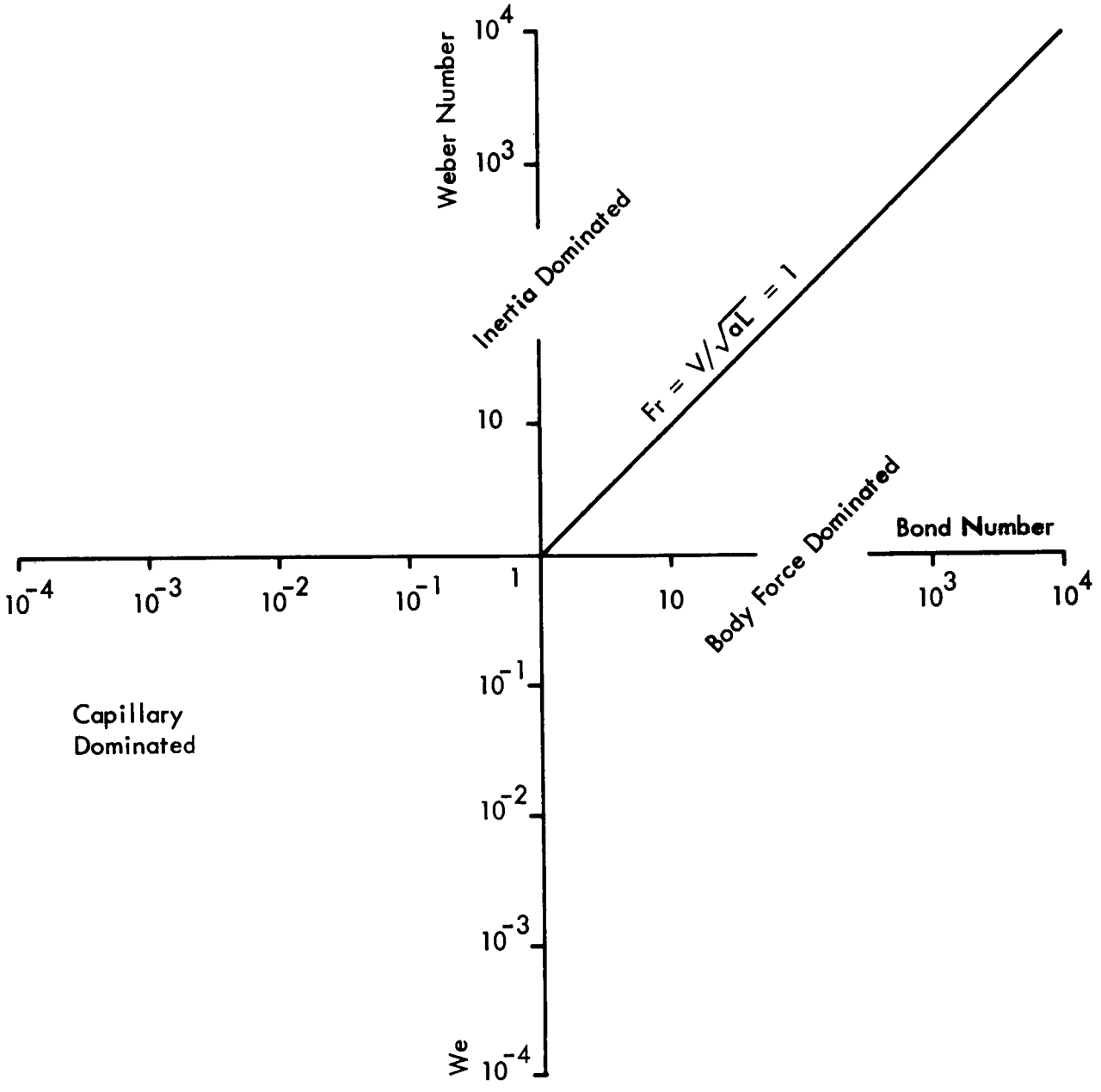

Figure 1 Hydrodynamic Regimes of Fluid Behavior

For an acceleration of 10^{-6} ge, Bo = 3.22 in a 10 ft radius tank of liquid hydrogen. Thus it is seen that the vehicle may not be considered to be in zero gravity but will be essentially in "low" gravity.

A. Behavior of Liquid Resulting from Initial Sloshing

Should the longitudinal acceleration of the container be reduced at the instant that the energy of the wave, as given by Eq. (6) is manifested as potential energy, the wave would not be amplified (i.e., the amplitude would remain the same). If, however, part or all of the energy of the wave is manifested as kinetic energy at the time of a sudden reduction in acceleration, the fluid will travel forward seeking an elevation at which the total energy appears as potential energy. A dimensionless number may be formed from the Froude number which is equivalent to the height, in tank diameters; the total liquid mass in the container can be raised by the energy in the slosh wave against the acceleration present after the reduction in acceleration (Ref. 18).

$$\frac{b}{D} = \frac{E_s g_o}{m a_2 D} = \frac{Fr^2}{2} \tag{30}$$

where:

g_o = conversion factor, 32.2 lb_m-lb_f^{-1} ft-sec^{-2}

b = jump height of liquid, ft

m = total mass of liquid in tank, lb_m

a_2 = longitudinal acceleration of tank after a change in acceleration, ft/sec^2

Fr = Froude number

For a cylindrical tank, assuming a flat (or equivalent curved) bottom from Eqs. (6) and (30):

$$\frac{b}{D} = \frac{0.176 \frac{a_1}{g_e} \zeta^2}{\frac{h_e}{D} D^2 \frac{a_2}{g_e}} \tag{31}$$

Should b/D significantly exceed the distance between the undisturbed liquid surface and the forward bulkhead of the tank, a circulatory motion will be created with the liquid flowing up one wall of the tank, across the forward bulkhead, down the other wall, etc. To gain some insight into the time necessary to regain control of the liquid, a means of estimating the duration of this motion is needed. Reynolds (Ref. 8) estimates the force due to eddy exchange in flowing fluids as:

$$Fe \approx \frac{\rho u^2 A}{g_o} \tag{32}$$

where:

Fe = force due to eddy exchange, lb_f

u = eddy velocity, ft/sec

A = wall area contacted by liquid, ft^2

The eddy velocity, u, is estimated in Reference 8 to be approximately one-tenth of the liquid velocity parallel to the wall, U. If it is also assumed that A is of the order of R^2,

$$Fe \approx \frac{0.01}{g_o} R^2 \rho U^2 \tag{33}$$

Applying Newton's second law:

$$\frac{-m}{g_o}\frac{dU}{dt} \approx \frac{0.01}{g_o} R^2 \rho U^2 \tag{34}$$

Integrating and solving for Δt,

$$\Delta t \approx \frac{100m}{\rho R^2}\left[\frac{1}{U_2} - \frac{1}{U_1}\right] \tag{35}$$

where:

Δt = time to reduce velocity from U_1 to U_2, sec

U_1 = velocity of liquid at beginning of damping, ft/sec

U_2 = velocity of liquid at end of damping time, ft/sec

The Reynolds number characterizing the flow may be estimated as follows. The velocity, V, is estimated by observing that the wave travels through a distance of 2ζ at the wall each half cycle; thus, $V = 4f_1\zeta$. The tank radius, R, is selected as the characteristic length. Then,

$$Re = \frac{4f_1 \zeta R\rho}{\mu} \tag{36}$$

Substituting Eq. (3) into Eq. (63),

$$Re = \frac{2R\rho}{\pi\mu}\left[\frac{2\alpha}{D}\left(\frac{a_1}{g_e}\right) g_e\right]^{1/2} \zeta \tag{37}$$

The Weber number may be estimated by assuming the same velocity and characteristic length as used for the Reynolds number.

$$We = \frac{\rho V^2 L}{\sigma} = \frac{16 f_1^2 \zeta^2 \rho R}{\sigma} = \frac{0.745\,\zeta_1^2}{\sigma/\rho}\left(\frac{a_1}{g_e}\right) g_e \tag{38}$$

The Bond number may easily be estimated, once the characteristic length is defined, by

$$Bo_R = \frac{aR^2}{\sigma/\rho} \tag{39}$$

B. Behavior of Liquid Resulting from Thermally Induced Propellant Motion

To determine whether the convective motion will cause the liquid to continue vertically upward when the acceleration is suddenly reduced at insertion into orbit, the Weber and Froude numbers must be calculated.

The Weber number can be calculated based upon the maximum boundary layer velocity, which is obtained by replacing X by h in Eq. (9), using R as the characteristic length. Thus:

$$We_R = \frac{\rho u_{1h}^2 R}{\sigma} = 13.83\,\frac{\rho R \nu^2 C^{5/7} h^{6/7}}{\sigma} \tag{40}$$

If We_R is substantially greater than unity, it may be assumed that the surface will break due to the dynamic force (Ref. 7).

The dimensionless height that the liquid may project forward under the low acceleration during orbital coast is determined by Eq. (30).

If the boundary layer kinetic energy is considered to affect the mass in the boundary layer, Eq. (30) becomes:

$$\frac{b}{D} = \frac{E_{BL} g_o}{m_{BL} a_2 D} \tag{41}$$

If all the kinetic energy due to convection is applied to the entire mass of liquid in the container,

$$\frac{b}{D} = \frac{(E_{BL} + E_D)\, g_o}{m\, a_2\, D} \tag{42}$$

C. Behavior of Liquid Resulting from Release of Stored Strain Energy

In a manner similar to that used above,

$$\frac{b}{D} = \frac{E_w g_o}{m a_2 D} \tag{43}$$

where E_w is the strain energy of the tank wall. Also, for strain energy stored in the liquid,

$$\frac{b}{D} = \frac{E_L g_o}{m a_2 D} \tag{44}$$

The Weber number may also be calculated to determine whether the liquid surface will be broken. The velocity that appears in the Weber number is calculated from

$$V = \sqrt{\frac{2 g_o E}{m}} \tag{45}$$

Then,

$$We = \frac{\rho V^2 L}{\sigma} = \frac{2 g_o \rho R E}{m \sigma} \tag{46}$$

where E may be E_w or E_L of Eqs. (23) and (24), depending upon which is of interest.

D. Persistence of Liquid Motion Due to Tank Draining

The height the liquid can rise against the acceleration of the space vehicle in orbit is, again,

$$\frac{b}{D} = \frac{E_{DR} g_o}{m a_2 D} \tag{47}$$

The Weber number may be calculated to determine whether the interface will break in the same way as under C. above.

V. ANALYSIS OF A SPACE VEHICLE STAGE

A discussion of the phenomena to be encountered in the propellant tanks of a space vehicle stage will be facilitated by basing the study on a typical stage and an assumed propellant tank venting and propellant settling system. It will then be relatively simple to extend the results to other stages that must perform similar missions.

A. General Description of the Space Vehicle Stage

A restartable third stage of a vehicle which injects a payload into a trans-lunar trajectory is considered. Propellants are liquid hydrogen and liquid oxygen loaded in an oxidizer-to-fuel ratio of 5.0. The main engine produces 200,000 lb of thrust at altitude. Total propellant loading is 240,000 lb. Figure 2 is a sketch showing the overall configuration and pertinent dimensions of the stage.

To avoid the need to resettle the propellants each time venting or engine restart is required, positive acceleration is provided from lift-off of the vehicle through orbital coast, to retain the liquid in a settled condition. Before the first ignition of the main engine of the stage, the acceleration is provided by solid propellant ullage rockets which are ignited at separation from the second stage and burn until the engine of the third stage has started. During orbital coast, the hydrogen tank is vented through longitudinally directed nozzles that provide a small thrust for propellant settling.

Eight liquid propellant auxiliary motors are arranged in two modules. Three motors in each module are used for attitude control during powered flight and orbital coast. The fourth motor in each module is used to settle propellants during damping of propellant motion at injection into orbit.

The liquid hydrogen tank is insulated from its external environment by a reinforced foam and from the liquid oxygen tank by an insulating common bulkhead. Approximately 3000 lb of liquid hydrogen are allowed for evaporation during 4-1/2 hours of orbital coast. The liquid oxygen tank is not insulated. Little oxygen

venting is anticipated, but should oxygen tank venting be required, a line directed through the center of mass of the stage has been provided.

A 100,000 lb payload is assumed. By assuming a stage mass ratio (ratio of total propellant capacity to stage dry weight) of 10, a stage dry weight of 24,000 lb is obtained. The propellant remaining at insertion into orbit is 2/3 of the original loading, or 160,000 lb. Thus, the vehicle acceleration just before insertion is approximately 0.70 ge (ge is defined here as an acceleration equal to that experienced by a body at the earth's surface due to gravity). Total liquid ullage motor thrust is 140 lb, giving an acceleration just after insertion of 5×10^{-4} ge. The net force provided by the vented hydrogen is a minimum of 5.7 lb, giving a minimum acceleration during orbital coast of 2×10^{-5} ge. A liquid depth-to-diameter ratio, he/D, for an equivalent cylindrical hydrogen tank (with a flat bottom) at insertion is 0.79. The equivalent L/D for a cylinder of equal volume is 1.25.

B. Analyses of Phenomena

If the phenomena identified in Chapter III cause liquid to impinge on previously dry surfaces of the interior of the hydrogen tank of the stage, a high rate of tank pressure rise is expected. The internal insulation surface will be heated by relatively warm pressurization gas during the first main engine firing. Calculations for the worst case, which assumes that the entire tank wall is covered by liquid hydrogen at insertion into orbit and all the heat from the tank wall evaporates liquid, predict that the tank pressure would rise by approximately 10 psi in 100 sec. (Ref. 19). Thus, it would be necessary to vent the tank to preclude the tank design limit pressure being reached. Therefore, liquid venting would occur if the propellant is in the vicinity of the vent inlet after approximately 100 seconds after insertion (main engine cut-off).

The analyses of individual phenomena that were given in Chapters III and IV will now be applied to the assumed stage. The objectives are to establish which of the phenomena have the potential to cause deleterious liquid motions and to suggest means of controlling the motion, where applicable.

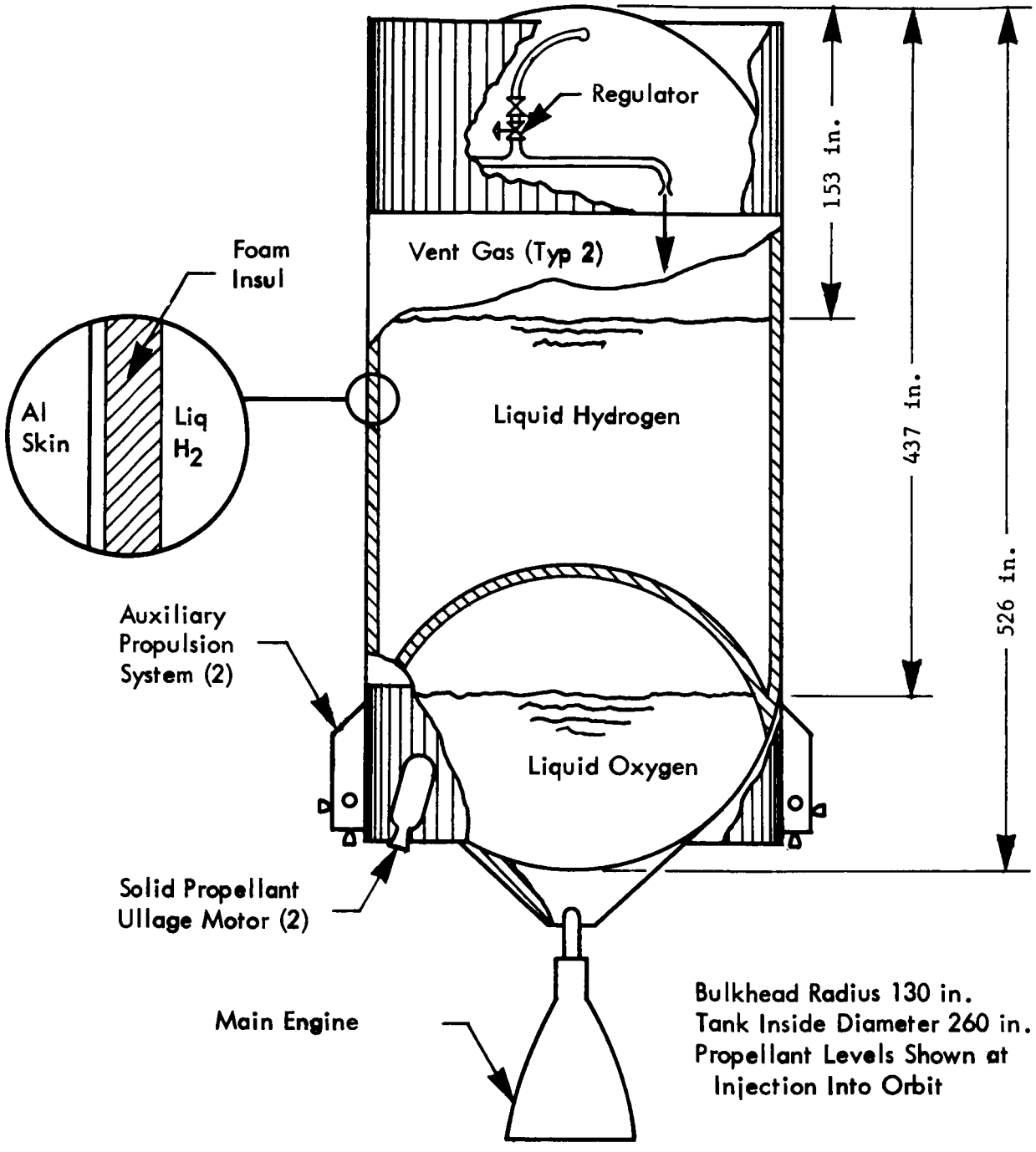

Figure 2 Configuration of the Restartable Third Stage

1. Sloshing Induced During Power Flight

To determine whether sloshing induced during powered flight has the potential to cause severe liquid motion, Eqs. (4), (5), (6), and (30) of Chapters III and IV will be applied to the space vehicle stage. For the first mode slosh wave, α in Eq. (5) is 1.84; he/D for the stage is 0.79. Thus,

$$K = \tanh 2\alpha \frac{h_e}{D} \approx 1$$

In Eq. (4), $\lambda \approx 1$ since the first mode slosh wave is of interest (Ref. 12). Thus,

$$\zeta_s = \frac{1}{2\alpha\lambda} \frac{D}{K} \approx 5.88 \text{ ft}$$

Substituting ζ_s for ζ in Eq. (6) to obtain the worst case, noting that a_1/ge is 0.70 and ρ for liquid hydrogen is approximately 4.4 lb_m/ft^3,

$$E_s = 0.553 \rho \frac{a_1}{g_e} R^2 \zeta_s^2 \approx 6960 \text{ ft-lb}_f$$

The surface energy due to sloshing is calculated from Eq. (7) to be only 7.09×10^{-3} ft-lb_f. This is negligible, and surface energy will, therefore, be eliminated from further consideration in this study.

Assuming, for simplicity, that the energy is distributed uniformly throughout the total hydrogen mass of 26,667 lb, at the acceleration just after insertion into orbit of 5×10^{-4} ge, Eq. (30) yields:

$$\frac{b}{D} = \frac{E_s g_o}{m a_2 D} = 24$$

Thus, just after insertion, there is adequate energy to drive the entire liquid hydrogen mass 24 tank diameters forward. Therefore, the propellant motion will be limited only by the confines of the tank (provided, of course, that the engine thrust is terminated at the instant this energy is manifested as kinetic energy of sloshing).

It may be, however, that this motion will not persist for the allowable period of time (estimated to be 100 sec based on tank pressure rise rate). To gain some insight into this, a response time order of magnitude estimate will be made using

Eq. (35). The initial velocity, U_1, will be estimated as was the velocity in Eq. (36), i.e., $U_1 = 4f_1 \ell_s$. The velocity to which the motion must be damped, U_2, is of the order of 0.1 ft/sec to avoid excessive jump heights at the final acceleration, 2×10^{-5} ge (Fig. 3). From Eq. (3), $f_1 = 0.312$ cycles/sec. Thus, $U_1 = 4f_1 \ell_s = 7.35$ ft/sec. Substituting the above data into Eq. (36), the damping time is estimated to be:

$$\Delta t \approx \frac{100m}{\rho R^2} \left(\frac{1}{U_2} - \frac{1}{U_1} \right) = 51{,}600 \text{ sec}$$

Thus, it is seen that, even if turbulent damping should persist, the damping time is several orders of magnitude greater than the available time. To determine whether turbulent flow will persist, the transition from turbulent to viscous flow is estimated to occur at a Reynolds number of the order of 1000.

$$Re = \frac{\rho R U}{\mu} = 1000$$

$$U = 1.83 \times 10^{-4} \text{ ft/sec}$$

where μ = dynamic viscosity of liquid hydrogen, 3×10^{-2} lb_m/hr ft (Ref. 20). Therefore, it may be concluded that turbulent flow will persist.

It is appropriate to consider previous experience with sloshing to determine if conditions approaching the worst case estimated above are normally encountered. An idea of the sloshing to be expected in the hydrogen tank may, perhaps, be gained by examining the Saturn I, S-IV stage flight data (Ref. 21). Data from flight SA-5 show evidence of hydrogen sloshing at both the first and second mode natural frequencies, approximately 0.4 and 0.7 cps. The maximum hydrogen slosh amplitude of 0.6 feet occurred 50 seconds after ignition of the S-IV stage and decayed to 0.13 feet in approximately 300 seconds. Similar results were obtained on the other Saturn I flights. From these data, it is concluded that the worst case estimate is probably too severe.

It seems reasonable to ask whether the sloshing for the stage considered herein can be predicted or estimated. It is beyond the scope of this study to make a slosh prediction for the assumed stage. An estimate, however, is possible, since

a prediction is available for a stage that differs from the assumed one only in the acceleration and in the amount of propellant remaining at insertion into orbit (Ref. 22). The stage considered in Reference 22 had an acceleration just before insertion of 3.5 ge. The predicted slosh wave had an amplitude of 0.42 feet and a frequency of 0.7 cycles/sec. The maximum liquid velocity occuring at the container wall was given as 1.83 ft/sec. If it is assumed that the kinetic energy associated with this wall velocity is converted into potential energy, it is found that the liquid can jump 100 feet at the acceleration of 5×10^{-4} ge (Fig. 3). Since this jump height is much larger than the distance from the liquid surface to the top of the tank, the vent inlet will be covered. If the jump height tolerated was arbitrarily set at a quarter of a tank diameter, an acceleration of 0.01 ge or 3000 lb thrust would be required on this stage (Fig. 3). The propulsion system required to produce such an acceleration for the duration required for the motions to subside would result in a severe weight penalty.

An apparent solution to the above problem would be to baffle the hydrogen tank to prevent these large slosh velocities. It was calculated (Ref. 23) that three ring baffles 10 inches wide, spaced 12 inches apart with the middle baffle located at the expected liquid level at injection into orbit would damp the maximum slosh velocity to 0.15 ft/sec. This would result in jump heights of 0.7 feet at 5×10^{-4} ge and 17 feet at 2×10^{-5} ge (Fig. 3). However, the prediction of a 17 foot jump appears conservative, since the kinetic energy dissipated during the 100 seconds of auxiliary engine firing and the deflection of the flow by the upper slosh baffle were not considered.

From the above, it is concluded that propellant sloshing formed during powered flight has the potential to create propellant motions during orbital coast that will interfere with propellant tank venting. Damping times are estimated to be excessive for the assumed stage. Slosh baffles are an applicable means of reducing the energy available to create propellant motion during orbital coast.

2. Thermally Induced Propellant Motion

To determine whether thermally induced propellant motion has the potential to cause liquid venting, the equations presented in Chapter III, part B will be

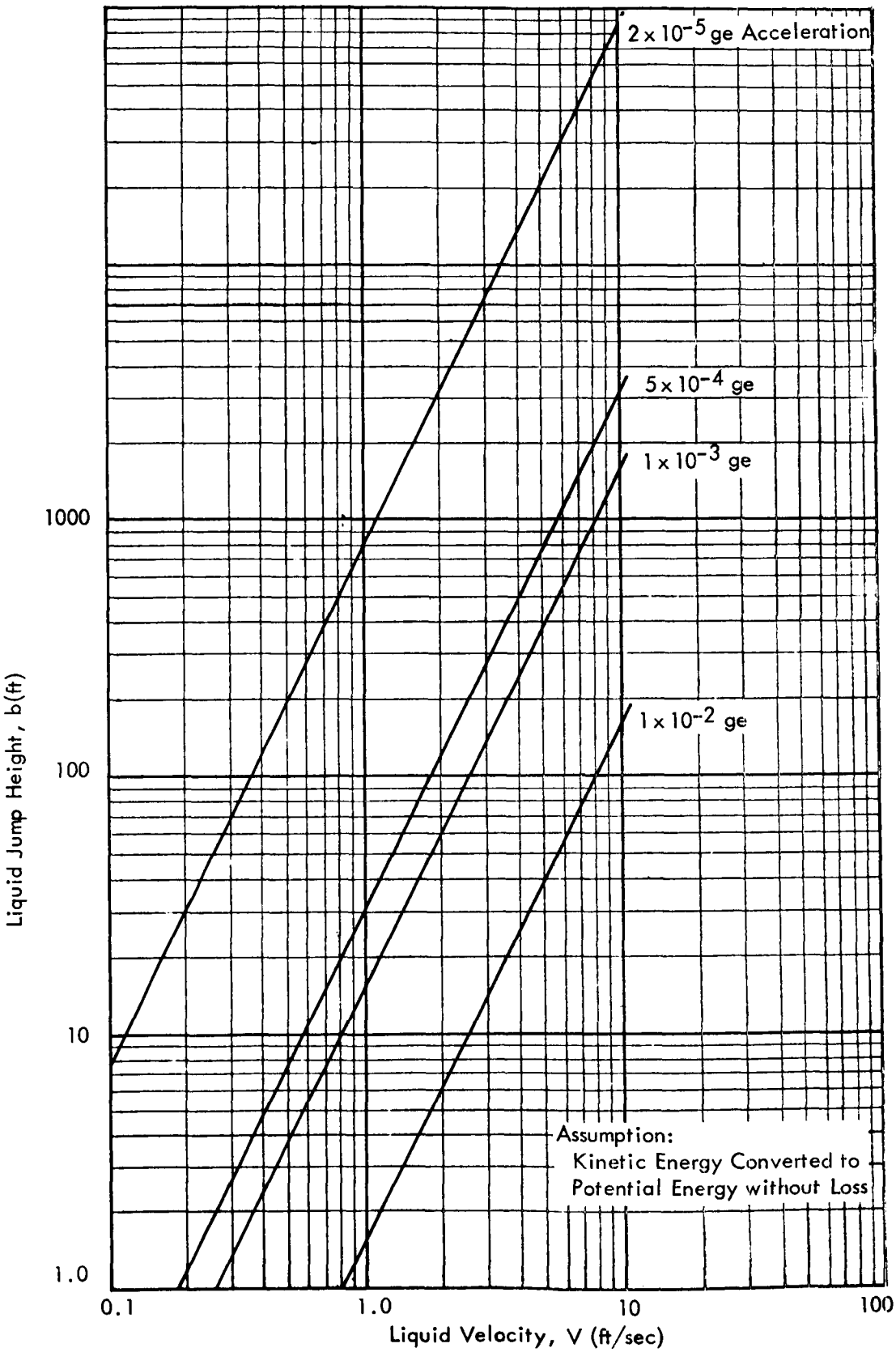

Figure 3 Liquid Jump Height at Various Low Gravity Conditions

applied to the assumed stage hydrogen tank. Common to all pertinent equations is the quantity:

$$C = \frac{a\beta\dot{q}_w}{\rho c_p \nu^3}$$

The symbols β, ρ, c_p, and ν refer to liquid properties. For liquid hydrogen, their values are (Refs. 20 and 24):

$\beta = 9.35 \times 10^{-3}$, R^{-1}

$\rho = 4.4$, lb_m/ft^3

$c_p = 2.3$, $Btu/lb_m\ R$

$\nu = 2 \times 10^{-6}$, ft^2/sec

The acceleration, a, will be assumed to be 0.7 ge, the cutoff acceleration of the assumed stage. The heat flux, $\dot{q}_w$, was given earlier as 0.08 $Btu/sec\text{-}ft^2$. (The analysis of Reference 14 used 1.0 ge as the average acceleration of a stage similar to the one assumed herein. This is considered arbitrary, however, and of small importance since the boundary layer equations contain the factor C to fractional powers in all cases.) From the above, for the assumed stage, $C = 2.1 \times 10^{14}\ ft^{-4}$. The other factor required to apply the equations is the maximum boundary layer run length, h. From Fig. 2, h = 23.67 ft.

The maximum boundary layer velocity may be calculated by replacing X with h in Eq. (9). Thus:

$$u_{1h} = 3.72\,\nu\,C^{5/14}\,h^{3/7} = 4.02 \text{ ft/sec}$$

From Fig. 3 at $a/ge = 5 \times 10^{-4}$, the acceleration during ullage engine firing, a jump height of 400 feet is read for a velocity of 4.02 ft/sec. For the continuous venting period ($a/ge = 2 \times 10^{-5}$) the jump height is 10,300 feet. Of course, there is only an infinitesimal mass at such a high velocity.

It might be more appropriate to consider the jump height for a case where the kinetic energy in the entire boundary layer is applied to the mass of liquid in the boundary layer.

From Eq. (14),

$$E_{BL} = \frac{0.061\pi D\rho v^2 C^{9/14} h^{18/7}}{2g_o} = 6.45 \text{ ft-lb}_f$$

The mass in the boundary layer, from Eq. (16) is:

$$m_{BL} = 0.307\pi D\rho C^{-1/14} h^{12/7} = 2000 \text{ lb}_m$$

Applying Eq. (41) for the period of ullage engine firing:

$$\frac{b}{D} = \frac{E_{BL} g_o}{m_{BL} a_2 D} = 0.297$$

and for the orbital coast, where $a/ge = 2 \times 10^{-5}$

$$\frac{b}{D} = \frac{E_{BL} g_o}{m_{BL} a_2 D} = 7.44$$

Thus, the entire mass in the boundary layer can easily be driven to the top of the forward bulkhead.

It has been established that 100 seconds can be allowed before tank venting is necessary. Thus, some mixing may take place. Neglecting damping, an indication of the liquid jump height after mixing may be obtained by applying the entire kinetic energy in the tank due to convection to the entire mass of liquid available. The kinetic energy in the boundary layer has been calculated. The kinetic energy in the downward core flow may be obtained from Eq. (22b):

$$E_D = \frac{\pi D\rho}{8g_o} [1.15^2 v^2 C^{4/7}] \sum_{i=1}^{h/\Delta x} \frac{X^{16/7} \Delta X_i}{[D - 2.105 C^{-1/14} X^{5/7}]}$$

To evaluate this equation, the tank was replaced by one of the same height but with a flat bottom. This will result in a calculated value for E_D that will be somewhat lower than will exist in reality. Ten increments of height were used ($h/\Delta x = 10$). The calculated value for E_D was 0.55 ft/lb$_f$. Thus, the total kinetic energy due to convection from Eqs. (14) and (22b) becomes $6.45 + 0.55 = 7.0$ ft/lb$_f$.

From Eq. (42) for the period of ullage engine firing:

$$\frac{b}{D} = \frac{(E_{BL} + E_D)\, g_o}{m a_2 D} = 0.0242$$

and for the orbital coast:

$$\frac{b}{D} = \frac{(E_{BL} + E_D)\, g_o}{m a_2 D} = 0.605$$

Thus, it is seen that initially, in an unbaffled tank, a very small mass may be expected to travel to the tank top. The slower moving fluid following this, however, will on the average "jump" less than about 0.3D, until auxiliary motor cutoff. Then, depending on the time required for turbulent mixing, the jump height will stabilize at about 0.6D. Viscous effects may be expected to reduce this final height with time.

To prevent liquid venting as a result of this phenomenon, it is only necessary to deflect the high velocity liquid in the boundary layer and promote mixing. A ring baffle of the type discussed earlier for the reduction of sloshing would appear applicable. The baffle should be at least as wide as the maximum boundary layer thickness, which from Eq. (10) is:

$$\delta_h = 0.526\, C^{-1/14}\, h^{5/7} = 0.479 \text{ ft}$$

3. Release of Stored Strain Energy

The potential of stored strain energy to cause deleterious liquid motion in the assumed stage may be assessed by applying Eqs. (23) and (24). First, the effect of strain energy stored in the tank wall will be considered. To do this, certain characteristics of the tank must be established. The following assumptions are made:

a. The tank is constructed of high strength aluminum.
   Y = modulus of elasticity = 10×10^6 lb_f/in^2 (Ref. 25).
   σ_y = yield stress = 56,000 lb_f/in^2 (Ref. 26).

b. The factor of safety (F.S.) is 1.4 based on the yield stress (assumption based on Ref. 26).

c. Hoop stress is the tank design criterion.

d. The tank design pressure is 40 lb_f/in^2 (Ref. 27).

Conventionally, then, for a thin wall cylindrical tank:

$$t = \frac{p\,D(F.S.)}{2\sigma y} = 0.13 \text{ in.}$$

To apply Eq. (23), it was also necessary to assume the tank pressure at insertion into orbit. A pressure of 26 psia was assumed. From Eq. (23), then

$$E_w = \frac{\pi R^3 \rho}{Yt}\left[\frac{\rho h^3}{3}\left(\frac{a_2^2 - a_1^2}{g_o^2}\right) + p_o h^2\left(\frac{a_2 - a_1}{g_o}\right)\right] = 840 \text{ ft-lb}_f$$

Assuming this energy is distributed to the total mass of liquid hydrogen, applying Eq. (43) for the period of ullage motor firing:

$$\frac{b}{D} = \frac{E_w g_o}{m a_2 D} = 2.9$$

and for the orbital coast where $a/ge = 2 \times 10^{-5}$:

$$\frac{b}{D} = \frac{E_w g_o}{m a_2 D} = 72.5$$

It is seen that tank wall strain energy, released by the reduction in hydrostatic pressure at insertion into orbit, is of a magnitude sufficient to cause chaotic liquid motion during ullage burn and orbital coast. The liquid motion would be expected to persist for an extended time in orbital coast, since the velocities would be of the same order as would be induced by the worst case of sloshing (the calculated values of b/D are of the same order). It is possible that the slosh baffles placed within the tank to reduce sloshing induced during boost would effectively attenuate this motion. The following elements of conservatism also exist:

a. The liquid may not respond in a gross manner to the tank wall vibration as the wall relaxes.

b. A portion of the released strain energy will be absorbed in internal damping by the tank wall and insulation.

c. Part of the strain energy will be manifested as vibrational energy of the payload, forward of the assumed stage, and of the engine and structure aft of the tank wall.

d. The tank volume will be reduced with a portion of the above energy going to ullage vapor compression.

The strain energy stored in the liquid in the tank and released by the reduction in hydrostatic head at insertion into orbit may be estimated from Eq. (24). Equation (24) is approximate at best since it was derived for a liquid contained within a flat-bottomed container. The liquid height, h, in Eq. (24) was replaced by an equivalent liquid height, $h_e = 0.79D$. This will cause Eq. (24) to yield a value of stored compression energy somewhat smaller than would actually exist. Values for all the quantities in Eq. (24) with the exception of β (the coefficient of isothermal compressibility of liquid hydrogen) have been given earlier. For hydrogen, $\beta = 7.44 \times 10^{-7}$ ft^2/lb$_f$ (Ref. 24). Applying Eq. (24) to the assumed stage:

$$E_L = \frac{\pi R^3 \rho \beta h^2 (a_2 - a_1)}{2g_o} \left[p + \frac{(a_1 + a_2)\rho h}{3g_o} \right] = 455 \text{ ft-lb}_f$$

Applying Eq. (44) for the time of ullage motor firing, assuming the energy E_L is applied to the total mass of liquid hydrogen in the tank:

$$\frac{b}{D} = \frac{E_L g_o}{m a_2 D} = 1.57$$

and during orbital coast:

$$\frac{b}{D} = \frac{E_L g_o}{m a_2 D} = 39.3$$

If this energy is converted to kinetic energy of the liquid, chaotic motion would result. Again, the liquid may simply expand, compressing the vapor in the ullage. The slosh baffles would tend to dampen the resulting motion.

4. Fluid Motion of Tank Draining

The kinetic energy of the liquid due to draining may not be calculated directly from Eq. (25) since the velocity distribution within the liquid is not known. If, however, in Eq. (25), v_e and v_r are assumed negligible, the mean value of v_x may be assumed equal to the fall rate of the liquid/vapor interface, and the lower limit of the kinetic energy due to draining established.

The specific impulse, Isp, of the engine is assumed to be 425 lb_f-sec/lb_m. Thus, for a 200,000 lb_f thrust, the total propellant flowrate is:

$$\dot{w}_T = F/I_{sp} = 470 \text{ lb}_m/\text{sec}$$

The liquid hydrogen flowrate is 1/6 of the above or 78.3 lb/sec. The interface fall rate is 0.048 ft/sec. From Eq. (25) then:

$$E_{DR} = \frac{mV^2_x}{2g_o} = 1.04 \text{ ft-lb}_f$$

During ullage motor firing, the equivalent jump height from Eq. (47) is:

$$\frac{b}{D} = \frac{E_{DR}g_o}{ma_2D} = 3.6 \times 10^{-3}$$

and during orbital coast:

$$\frac{b}{D} = \frac{E_{DR}g_o}{ma_2D} = 0.09$$

The above values of b/D are negligible in comparison with those calculated earlier for other phenomena. Thus, this phenomenon will not be considered further.

VI. FEASIBILITY OF EXPERIMENTS

The feasibility of experiments to investigate the phenomena described in the preceding chapters depends on the availability, or possibility of constructing, facilities which can produce usable low gravity test time.

A significant limitation of any low gravity test facility is the level of extraneous distrubances introduced by the test facility. It is imperative to have controlled conditions for the low gravity fluid dynamics experiments. A reasonable criterion is that the liquid-vapor interface must be stable under the influence of facility-induced disturbances. From Reference 9 the liquid-vapor interface is stable for accelerations directed from the more dense to the less dense fluid if, for a liquid which has a contact angle with the container wall of zero, $Bo \leq 0.8423$. The "critical" acceleration, a_c, defined as the acceleration where $Bo = 0.8423$, has been plotted versus tank radius in Fig. 4.

A. Test Facilities

The following are descriptions of the various facilities for low gravity fluid mechanics testing and their capabilities and limitations.

1. Aircraft

An extensive low gravity fluid mechanics test program utilizing airplanes flying low gravity trajectories was undertaken (Ref. 28). To accomplish the nominally zero gravity maneuver, the airplane is first put into a dive. It is then pitched up. The pilot then flies a nominally zero gravity Keplerian trajectory, applying thrust to overcome drag until the airplane must again pitch up to recover from the maneuver. The following table lists capabilities of several aircraft for low gravity testing with experiment packages free floating and attached to the aircraft. Size of the free floating packages is limited to allow for package drift in the cargo space.

TABLE II

AIRCRAFT CAPABILITIES FOR LOW GRAVITY TESTING

Aircraft	Test Cond.	Test Time (sec)	Accel. Experienced (ge)	Experiment Size (in)
B-57	Theoret. Max.	57		
	Free Float	3-5	10^{-4}	6 (cube)
	Attached	30-40	10^{-2}	30 (cube)
AJ-2	Theoret. Max.	40		
	Free Float	8-15	10^{-4}	24 (cube)
	Attached	15-30	10^{-2}	48 (cube)
C-130	Theoret. Max.	34		
	Free Float	8-15	10^{-4}	48 (cube)
	Attached	15-30	10^{-2}	100 (cube)
X-15	Theoret. Max.	200	0.03	8(dia) x 60 cylinder 20 x 24 x 14 box 22 x 33 x 33 box

Two types of disturbances are present in aircraft testing, those occurring before entering the nominally zero gravity trajectory, and those occurring during the "zero gravity" period. Before entering "zero gravity," a 1.5 to 2.5 ge pitch-up of the aircraft is required at a rate of approximately 8 deg/sec. The acceleration direction is known, thus the experiment might be oriented to avoid disturbing the liquid-vapor interface in the container. The rotation, however, causes circulation of the fluid. The accelerations listed in Table II are random in direction, thus can disturb the interface. Therefore, for the B-57, for example, from Table II and Fig. 4,

	Theoret. Max.	Float	Attached
Test Time (sec)	57	3-5	30-40
Available Space for Experiment (in)		6	30
Acceleration Level (ge)		10^{-4}	10^{-2}
Practical Container Diameter (in)		6	1
Test Fluid	———	Water	———

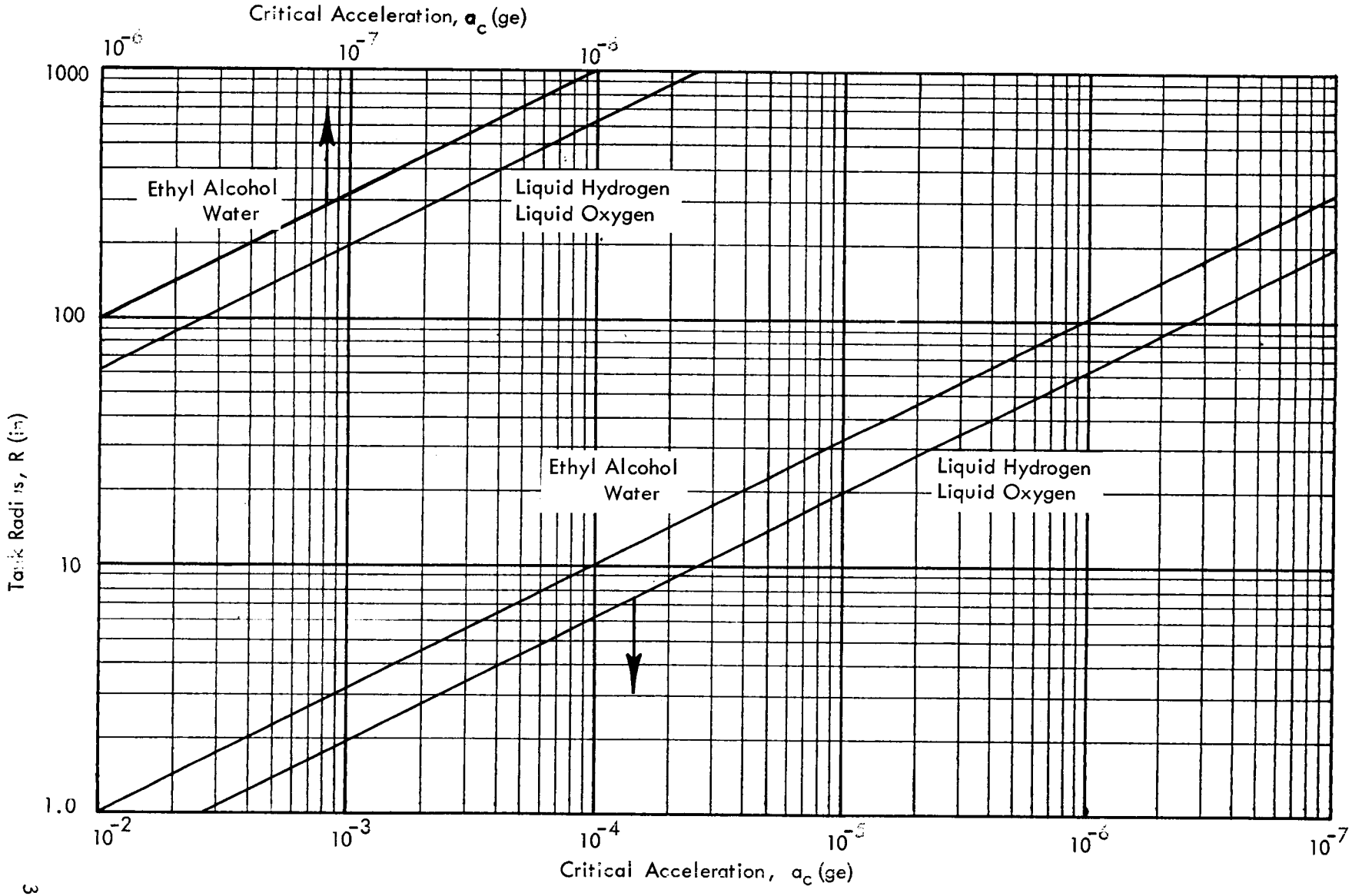

Figure 4 Container Size for Interface Stability as a Function of Acceleration

It is seen that difficulties may be anticipated in scaling from container diameters of this order to those of space vehicle propellant tanks that are one to three orders of magnitude larger, and from test times of several seconds to space vehicle coast times of several hours.

2. Drop Tower

Drop towers have been used extensively for low gravity fluid mechanics and heat transfer experimentation. Data have been obtained on boiling heat transfer, static liquid-vapor interface shape and formation time, and sloshing. Available drop facilities utilize a free-fall distance of 35 to 100 feet, which results in a drop time of 1.5 to 2.5 seconds. A study was made to determine the feasibility of a drop tower to increase the free-fall time to 4.5 sec (320 ft) (Ref. 29). It was found that a maximum experiment disturbance of 10^{-4} ge could be obtained with a drag shield having a ratio of mass to product of drag coefficient and frontal area (m/C_DA) of 1000 lb_f/ft^2. This means that an aerodynamically-shaped body of about 2800 pounds would be required as a drag shield. An experimental package of about 200 pounds would be housed in a 36 inch diameter container falling within the drag shield. Many design problems were identified, the most important of which was the means of stopping the heavy drag shield without damage when it reached the end of the drop, but none were thought to be insurmountable.

3. Drops from Balloons

The feasibility of dropping low gravity experiments from balloons at high altitudes was investigated (Ref. 30). This would be similar to using a drop tower, except that an increase in free-fall time would be gained by virtue of the altitude of the starting point. Also, atmospheric drag would be lower in the less dense atmosphere at, say, 100,000 feet than near sea level (100,000 feet is the design float altitude of an available balloon). Briefly, this scheme was found to be impracticable because of windage and because for the same longitudinal travel of an experiment within a drag shield (6.5 ft), less than one second more free fall time would be obtained than in a 320 ft. drop tower.

4. Rocket Vehicles

Rocket vehicles have no fundamental limitations on their capability for zero and low gravity fluid mechanics and thermal testing since essentially any test time and experiment size can be obtained and the vehicle can be accelerated in any direction at any level desired. Thus, small, relatively low cost sounding rockets would seem to offer an appropriate facility for subscale testing. While small sub-orbital rockets are subject to some of the same limitations as airplanes, the limitations are less severe because available test times are longer and random accelerations are lower. A survey was made of available sounding rockets (Ref. 29). Data were obtained on the WASP I, WASP II, Scout, Athena, Aerobee, and pods mounted on Atlas intercontinental ballistic missiles. The WASP I may be considered representative, its available "zero gravity" time is 7 to 11 minutes with random accelerations below 10^{-5} ge. This would allow a test tank of 20 to 32 inch diameter based on the interface stability criterion (Fig. 4).

B. Analysis of Experiments

In this section, the phenomena identified earlier will be examined to determine the possibility of simulating them in subscale experiments. The simulations will be based on the conditions estimated for the space vehicle stage.

1. Sloshing Induced During Powered Flight

To assess the possibility of investigating this phenomenon in subscale tests, it is necessary to first calculate the values of the scaling parameters, b/D ($=Ego/ma_2D$), We_R, and Bo_R for the assumed full-scale stage. The conditions at the intermediate acceleration level, 5×10^{-4} ge, will not be calculated, since this acceleration will be assumed to have the sole effect of shifting the wave phase between the high and low acceleration phases (Ref. 31).

Several cases will be considered: (1) the worst case of sloshing where $E_s = 6960$ ft-lb_f; (2) a case where the wave amplitude is the same for this stage as for the stage of Reference 22 ($\zeta = 0.42$ ft); and (3) a case where the slosh wave energy remains the same for this stage as for the stage of Reference 22.

Table III, page 41, gives the values of the dimensionless scaling parameters calculated for the assumed full-scale stage from Eqs. (6), (30), (37), (38) and (39). Pertinent values are shown for two times, main engine firing ($a/ge = 0.70$) and orbital coast with continuous venting ($a/ge = 2 \times 10^{-5}$).

To conduct a subscale test to investigate this phenomenon, it is necessary to use a container large enough to easily measure the wave amplitude. Further, during the low acceleration phase of the test, the imposed acceleration must be larger than the random acceleration imposed by the test facility. It must also be possible to examine at least one cycle of liquid motion. The liquid slosh motion may be set up at $a/ge = 1.0$ for the drop tower. For the airplane, it will be assumed that the slosh motion is formed during a pull-up at $a/ge = 2.5$. The modified Froude number, b/D, will be assumed to be the primary parameter to be modeled; We_R, Bo_R, and Re_R will be checked to assure they are in the desired regime (as defined by Fig. 1) to simulate the full scale space vehicle stage conditions.

It is desirable to have the maximum wave energy before the release into low gravity to avoid the need for extremely low acceleration during the test. Thus, in Eq. (6), the slosh amplitude, ζ, is specified as being equal to ζ_s. The first mode slosh wave is assumed; thus, $\lambda \approx 1$ and $\alpha = 1.84$ in Eq. (4).

The following equations are derived for the above conditions. Equation (31) is:

$$\frac{a_2}{ge} = \frac{0.176\, a_1/g_e}{\frac{Ego}{ma_2D}\,\frac{h}{D}} \left(\frac{\zeta}{D}\right)^2$$

From Eq. (4) $\frac{\zeta_s}{D} = \frac{1}{2\alpha\lambda} = 0.277$ for $h/D = 0.79$. Thus,

$$\left(\frac{a_2}{ge}\right)_{max} = \frac{1.35 \times 10^{-2}\, a_1/g_e}{\frac{Eg_o}{ma_2D}\,\frac{h}{D}} \qquad (48)$$

where $(a_2/ge)_{max}$ is the largest acceleration during the test which can give the

TABLE III

SLOSH SCALING PARAMETERS FOR THE FULL SCALE STAGE

	a/ge	Bo_R	ℓ(ft)	E(ft-lb_f)	b/D	Re_R	We_R
Before Main Engine Cutoff	0.70	26.3×10^5			-		
Worst Case Slosh Wave	0.70	26.3×10^5	6	6960	-	9.2×10^7	2.4×10^5
Retain Amplitude of 3.5 ge stage	0.70	26.3×10^5	0.42	33.6	-	2.9×10^6	2.9×10^3
Retain Wave Energy of 3.5 ge stage	0.70	26.3×10^5	-	168	-	6.2×10^6	5.6×10^3
After Main Engine Cutoff	2×10^{-5}	75.2	-				
Worst Case Slosh Wave	2×10^{-5}	75.2	-	6960	675	9.2×10^7	2.4×10^5
Retain Amplitude of 3.5 ge stage	2×10^{-5}	75.2	-	33.6	2.96	2.9×10^6	2.9×10^3
Retain Wave Energy of 3.5 ge stage	2×10^{-5}	75.2	-	168	14.75	6.4×10^6	5.6×10^3

specified b/D. The Bond number based on tank radius is given by Eq. (39) as:

$$Bo_R = \frac{R^2 \rho a}{\sigma}$$

During the test, $a = a_2$. The maximum acceleration is given by Eq. (48). Combining Eqs. (48) and (39):

$$Bo_{R2} = \frac{3.38 \times 10^{-3} D^2}{\sigma/\rho} \left[\frac{a_1/g_e}{\frac{Eg_o}{ma_2 D} \frac{h}{D}} \right] \tag{49}$$

The Weber number, from Eq. (38) is:

$$We_R = \frac{16 f^2 \zeta^2 \rho R}{\sigma}$$

Substituting for ζ the value of ζ_s found above and equation (2) for f_1 wherein Bo_R is found from Eq. (49) and $\tanh(2\pi h/D) \approx 1$:

$$We_{R/max} = 5.74 \times 10^{-2} \left[\frac{a_1}{ge} g_e D^2 \right] \left[1 + \frac{13.57 \frac{\sigma}{\rho}}{D^2 \frac{a_1}{ge} g_e} \right] \frac{\rho}{\sigma} \tag{50}$$

This is the maximum Weber number that can be generated in the test. Equation (2) was used for f_1 because it is not known in advance that Bo_R will be large for the test condition.

From Eqs. (36) and (2), substituting ζ_s for ζ,

$$Re_R = 0.1696 \frac{D^2 \rho}{\mu} \left[\frac{1}{D} \frac{a_1}{ge} g_e \right]^{1/2} \left[1 + \frac{3.4}{Bo_{R_1}} \right] \tag{51}$$

The damping time is found from Eq. (35) by assuming that b/D is desired to be D/4 at the end of damping and realizing that the initial velocity, U_1, may be approximated by:

$$U_1 = \sqrt{2 a_2 D \left(\frac{Eg_o}{ma_2 D} \right)}$$

which is the same as Eq. (45). Further, an equivalent flat bottom container is assumed so that $m = \pi D^2 h_e \rho/4$. Then:

$$\Delta t = 314.2\, D \frac{h_e}{D}\left[\frac{2}{\sqrt{2a_2 D}} - \frac{1}{\sqrt{\frac{2Eg}{ma_2 D}}\; a_2\, D}\right] \tag{52}$$

The time for one cycle of liquid motion is calculated by dividing the initial liquid velocity, U_1, by the distance up one side, across the top, down the other side, and across the bottom of the container, then:

$$\tau = \frac{5.91\left[\frac{L}{D} + 1\right]}{\left[\frac{1}{D}\left(\frac{a_1}{ge}\right) ge\right]^{1/2}} \tag{53}$$

For the experiments, water is assumed to be the test fluid. Selecting the B-57 as a representative airplane, a practical container diameter is 4 inches (staying well within the 6 inch limit). For a drop tower test, a maximum container diameter is 20 inches; however, a 6 inch diameter container may also be considered.

Figure 5 summarizes results of calculations using Eqs. (48) through (53) for the conditions indicated above.

Comparing Fig. 5 and Fig. 1, it is seen that in any case considered (4 inch container, airplane test; 6 inch container, drop tower test; and 20 inch container, drop tower test) the fluid will be inertia dominated during the low gravity portion of the test because of the large values of We_R and Re_R. This is the desired condition as indicated by the values of We_R and Re_R given in Table III. It is not possible, however, to simulate b/D = 675 (the worst case) in any of the facilities considered, since $(a_2/ge)_{max}$ is lower than the minimum acceleration obtainable in any facility. The other values of b/D (=Ego/ma_2D) of interest ($b/D \leq 15$) can be obtained reliably. Further, in any case considered, τ is less than the available test time so that at least one cycle of liquid motion can be observed. It is obvious from the calculated values of Δt, however, that unless the method used to estimate Δt yields values too high by some 3 orders of magnitude, only the initial fluid

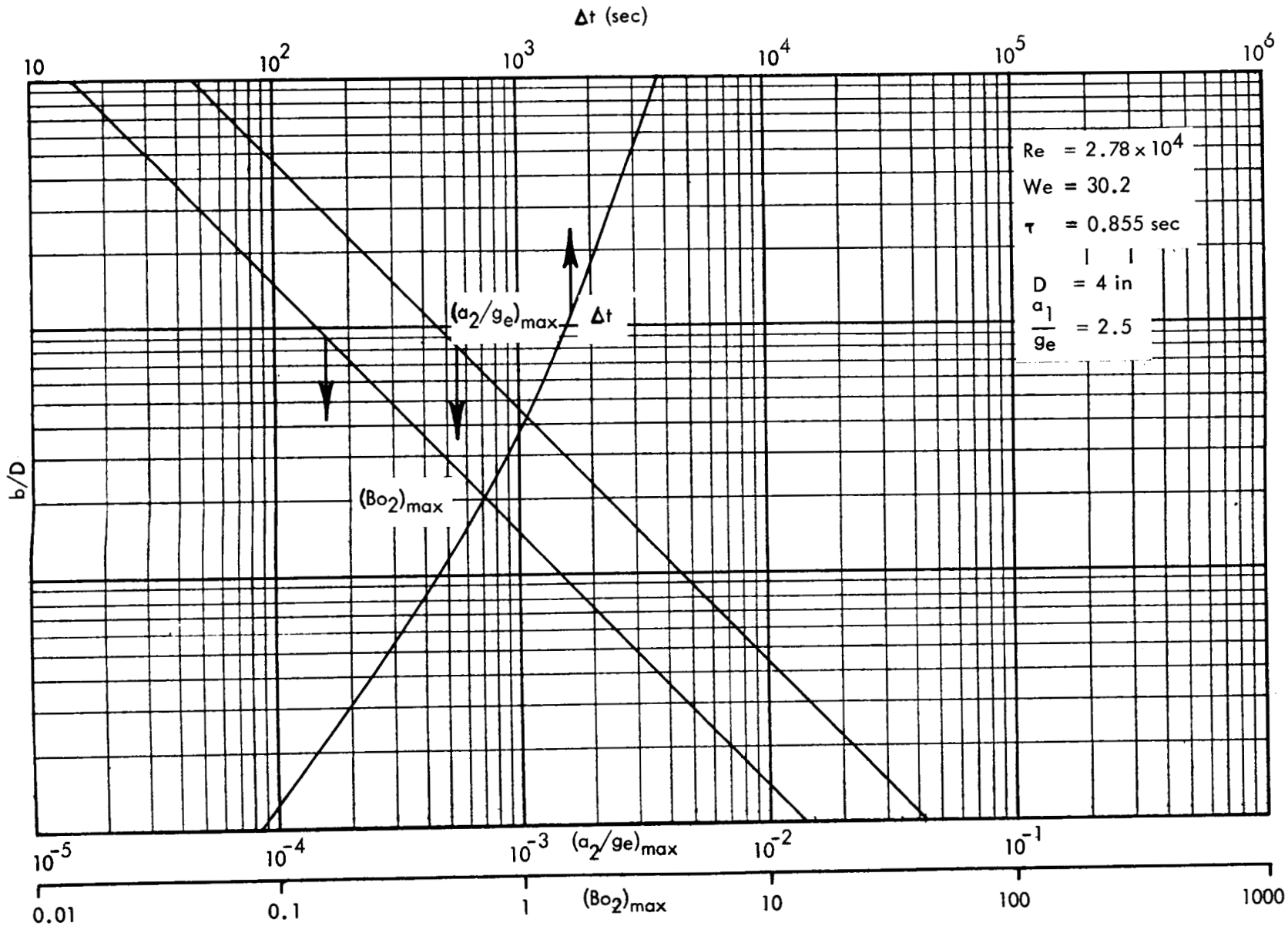

Figure 5a Slosh Parameters in an Airplane Test

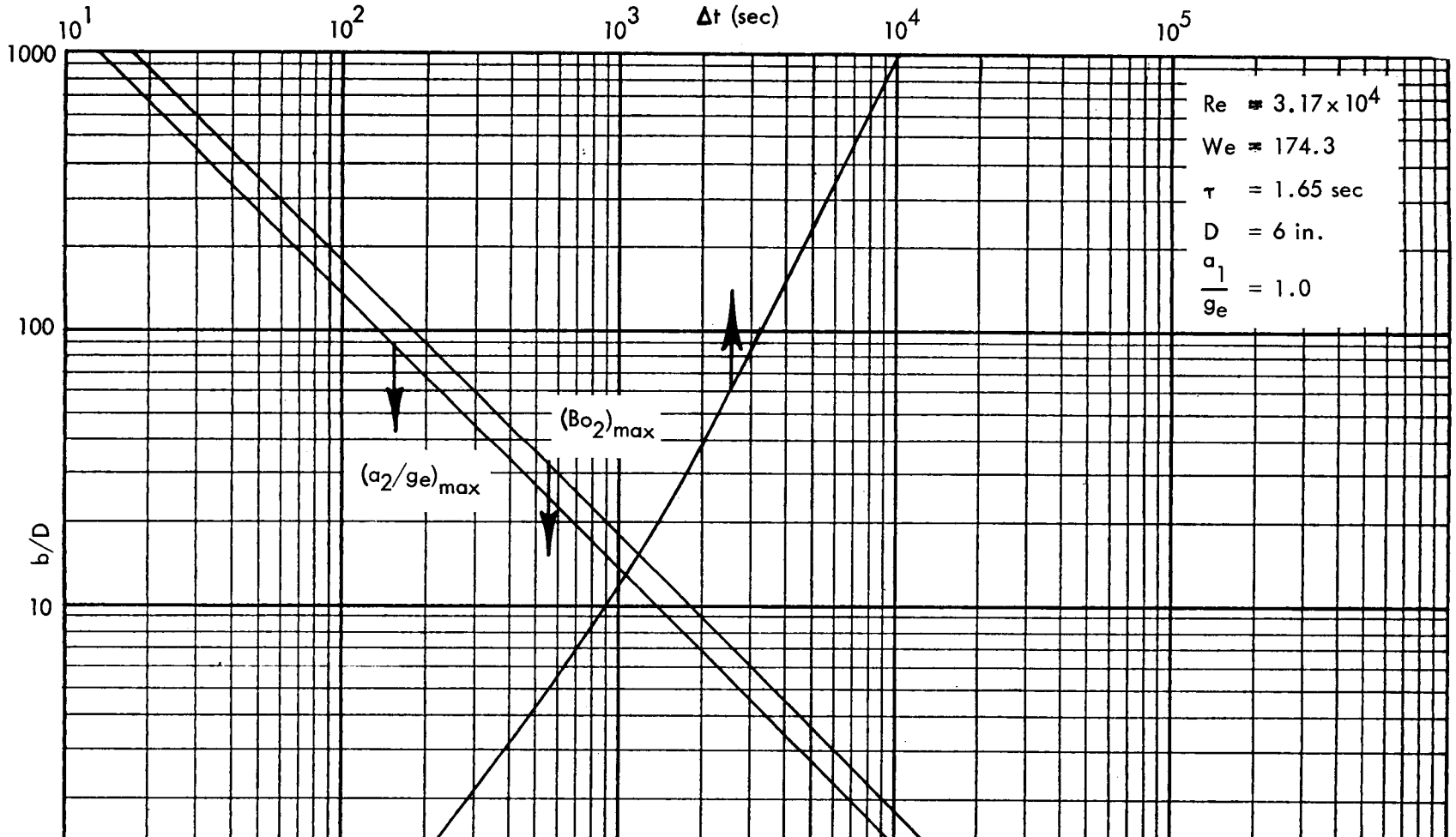

Figure 5b Slosh Parameters in a Drop Tower Test

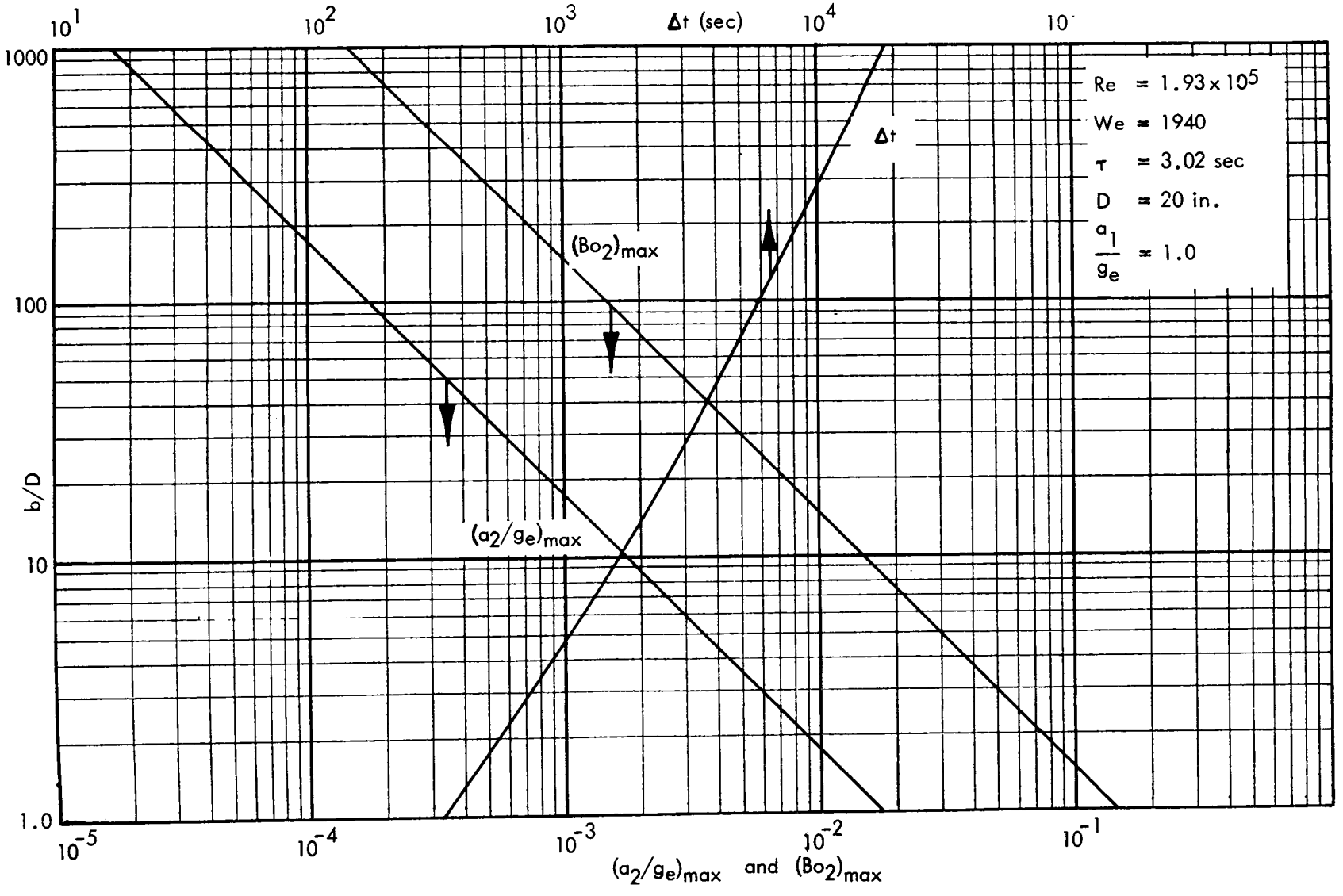

Figure 5c Slosh Parameters in a Drop Tower Test

motion can be observed in any subscale test short of one using a rocket vehicle. Furthermore, the limited controllable low-gravity time available in a sounding rocket test (7-11 minutes) limits the test container size to about 4 inches diameter as can be seen from the values of Δt shown in Fig. 5.

Consideration of other test fluids would be futile, since fluid properties do not appear in Eq. (53). Thus, the preliminary conclusion is drawn from consideration of this one phenomenon alone, the persistence of slosh induced during boost, that an orbital experiment may well be required.

2. Thermally-Induced Propellant Motion

To determine the possibility of simulating thermally-induced propellant motion as it would occur in the scale stage, We_R must be calculated for the stage. The other two significant parameters, Bo_R and b/D are given in Table III and in the text of Chapter IV. We_R may be calculated from Eq. (40):

$$We_R = \frac{13.83 \rho R \nu^2 C^{5/7} h^{6/7}}{\sigma} = 1.53 \times 10^5$$

Thus We_R is calculated to be so great that the interface will break and liquid motion will be dominated by dynamic forces.

The feasibility of subscale testing for the investigation of this phenomenon may be examined in a manner similar to that used in the section on boost slosh. Water will be assumed as the test fluid. A heat flux corresponding to the maximum for natural convection of 8×10^3 Btu/hr-ft^2 (Ref. 32) will be used. Since the formation time of the boundary layer is not known, only a drop tower test will be considered. Then, for two test containers of 6 inch and 20 inch diameter, the parameters of Table IV are calculated from Eqs. (9), (10), (14), (16), and (22b), and the definition of the modified Rayleigh number ($Ra^* = X^4 a \beta \dot{q}_w \rho c_p / \nu k^2$ (Ref. 22)).

To establish that a subscale test will yield useful data, it must be shown that the time of the intermediate acceleration can be simulated with a very small portion of the total available low gravity test time, or it must be assumed that the short period at the intermediate acceleration has little effect on the total fluid motion.

TABLE IVa

NATURAL CONVECTION PARAMETERS IN SIX INCH TEST TANK

Title	Symbol	Units	Value
$a\beta\dot{q}_w/\rho c_p \nu^3$	C	ft^{-4}	7.15×10^{12}
Acceleration before drop	a/ge		1.0
Boundary layer run length	h	ft	0.545
Modified Rayleigh number	Ra*		4.7×10^{11}
Maximum boundary layer velocity	u_{1h}	ft/sec	0.439
Maximum boundary layer thickness	δh	ft	0.0411
Kinetic energy in boundary layer	E_{BL}	ft-lb	5.21×10^{-5}
Kinetic energy, downward core flow	E_D	ft-lb	4.32×10^{-6}
Mass of fluid in boundary layer	m_{BL}	lb	1.28

TABLE IVb

NATURAL CONVECTION PARAMETERS IN A TWENTY INCH TEST TANK

Title	Symbol	Units	Value
$a\beta\dot{q}_w/\rho c_p \nu^3$	C	ft^{-4}	7.15×10^{12}
Acceleration before drop	a/ge		1.0
Boundary layer run length	h	ft	1.82
Modified Rayleigh number	Ra*		5.9×10^{13}
Maximum boundary layer velocity	u_{1h}	ft/sec	0.709
Maximum boundary layer thickness	δh	ft	0.0917
Kinetic energy in boundary layer	E_{BL}	ft-lb	3.88×10^{-3}
Kinetic energy, downward core flow	E_D	ft-lb	3.21×10^{-4}
Mass of fluid in boundary layer	m_{BL}	lb	34.0

First, examining the former, if the fluid is considered to flow around the inside of the forward bulkhead as a result of the initial maximum upward velocity of the boundary layer, a container of no more than 6 inches diameter is allowed in order to observe this initial phenomenon in 2 seconds or less (Eq. 53). This would leave only 2.5 seconds to observe the remainder of the motion. Therefore, it is possible by this criterion that the initial phase of the simulated intermediate acceleration period might be observed in a drop tower size container.

Second, it is assumed that the motion after some time is independent of the motion during the short period of the intermediate acceleration. The phenomena occurring during the long, very low acceleration period will be examined. It is desired to simulate two values of b/D as expressed by Eq. (30). First, the kinetic energy of the boundary layer, E_{BL}, is applied with the mass of liquid in the boundary layer. During the low acceleration period:

$$\frac{b}{D} = \frac{E_{BL} g_o}{m_{BL} a_2 D} = 7.44$$

Thus, to achieve the simulation,

$$\frac{a_2}{ge} = \frac{1}{7.44} \frac{g_o}{ge} \frac{E_{BL}}{m_{BL} D}$$

Similarly, applying the total kinetic energy due to convection and the total liquid mass in the tank:

$$\frac{a_2}{ge} = \frac{1}{0.605} \frac{g_o}{ge} \frac{(E_{BL} + E_D)}{m D}$$

The Bond number during the test is simply Bo_R evaluated at an acceleration of a_2, or, for the former case:

$$Bo_R = \frac{a_2}{ge} \frac{ge R^2}{\sigma/\rho} = \frac{1}{7.44} g_o \frac{E_{BL} R}{2 m_{BL} \frac{\sigma}{\rho}}$$

and for the latter case:

$$Bo_R = \frac{1}{0.605}\, g_o\, \frac{(E_{BL} + E_D)\, R}{2m\, \frac{\sigma}{\rho}}$$

The Weber number may be calculated from Eq. (40) and the data from Table IV. The following table summarizes conditions after the drop required to simulate the required values of b/D for the 6 inch and 20 inch containers, as calculated from the above expressions.

TABLE V

NATURAL CONVECTION SIMULATION

Tank Diameter	6 in.	6 in.	20 in.	20 in.
b/D Simulation	Boundary Layer	Entire Tank	Boundary Layer	Entire Tank
b/D	7.44	0.605	7.44	0.605
a_2/ge (drop)	1.1×10^{-5}	3.8×10^{-5}	0.92×10^{-5}	2.3×10^{-5}
Bo_R (drop)	3.3×10^{-2}	0.11	0.31	0.78
We_R	9.1	9.1	79	79

It is seen that the drop tower does not have the capability to simulate these conditions since an acceleration less than 10^{-4} ge is required in each case and the drop tower package can not achieve accelerations less than 10^{-4} ge. Furthermore, the Bond numbers calculated are in the surface tension or capillary dominated regime, and the liquid-vapor interface would be highly curved. Weber numbers are such, however, that if the required acceleration could be achieved, the surface could be expected to break (Ref. 33).

It is concluded that it is very doubtful that these liquid disturbances due to convection can be meaningfully investigated in small-scale tests.

3. Release of Stored Strain Energy

The feasibility of simulating the stage conditions for release of stored strain energy may be examined in the same manner as used earlier. First, the energy

stored in the tank wall will be considered. The transition time from the high to the low acceleration period appears critical, thus, only drop tower testing will be considered. Equation (23) is:

$$E_w = \frac{-\pi R^3 \rho}{Yt}\left[\frac{\rho h^3}{3}\left(\frac{a_2^2 - a_1^2}{g_o^2}\right) + p_o h^2\left(\frac{a_2 - a_1}{g_o}\right)\right]$$

Noting that the minimum acceleration available in the drop tower (10^{-4} ge) is negligible in comparison to the acceleration (1 ge) before the drop), Eq. (23) becomes:

$$E_w = \frac{\pi R^3 \rho}{Yt}\left[\frac{\rho}{3} h^3 \frac{a_1^2}{g_o^2} + p_o h^2 \frac{a_1}{g_o}\right] \tag{54}$$

The mass of liquid in the test tank is:

$$m = \pi \rho R^2 h_e \tag{55}$$

where h is the total liquid depth (1.09D from Fig. 2), and h_e is the equivalent liquid depth to yield the correct liquid volume ($h_e = 0.79\,D$ from the description of the stage). Substituting Eqs. (54) and (55) into Eq. (30) and solving for a_2/ge:

$$\frac{a_2}{ge} = \frac{1.505\,R}{Yt\,(b/D)}\left[0.727\,R\rho\,\frac{g_e}{g_o} + p_o\right] \tag{56}$$

This is the necessary value of a_2/ge that must be obtained to simulate the desired value of b/D.

The time that it is possible to simulate in the subscale test may be calculated quite simply from:

$$\tau_p = \tau_m \frac{Lp}{Lm} \frac{Vm}{Vp} \tag{57}$$

where:

Lp = characteristic dimension of assumed stage tank, ft

Lm = characteristic dimension of model tank, ft

Vp = characteristic velocity of liquid in stage tank, ft/sec

V_m = characteristic velocity of liquid in model tank, ft/sec

τ_p = simulated stage time, sec

τ_m = model test time (duration of drop), 4.5 sec

The velocities in Eq. (57) may be calculated from Eq. (45).

Reference 16 gives properties of several materials for test tanks. These properties are reproduced below:

	Modulus of Elasticity (lb/in^2)	Ultimate Stress (lb/in^2)
Glass-Borosilicate	6.8×10^6	1000
Polyethylene	2×10^4	1400
Polyvinyl Chloride	4×10^2	1000

The values of b/d that are to be simulated are 2.9 and 72.5 which occur on the assumed stage during auxiliary motor firing and during orbital coast, respectively.

If, in Eq. (56), the minimum value of a_2/ge is fixed, it is seen that t varies inversely with Y. The material thickness, t, may not be reduced without limit, since the stress to which the tank wall will be subjected during the test must be considered. The hoop stress at the tank bottom, neglecting the end effect introduced by the bottom, dictates a minimum wall thickness of:

$$t_{min} = \frac{R\overline{FS}}{\sigma_u}\left[p_o + \rho h \frac{a_s}{g_o}\right] \tag{58}$$

where:

t_{min} = minimum allowable wall thickness

$\overline{FS}$ = factor of safety based on ultimate stress

σ_u = ultimate strength of the tank material

a_s = stopping acceleration at the end of the drop

The above must be expressed in consistent units; the other symbols were defined earlier.

The longitudinal stress in the tank wall, assuming the tank is supported at the juncture of the cylindrical wall and the forward bulkhead dictates a minimum

wall thickness of:

$$t_{min} = \frac{\frac{R\overline{FS}}{\sigma_u}\left[p_o + \rho h_e \frac{a_s}{g_o}\right]}{2 - 2.44 \frac{D\rho_w}{\sigma_u}\frac{a_s}{g_o}} \qquad (59)$$

(consistent units)

If the stopping acceleration at the end of the drop, a_s, is assumed to be 20 ge, the package would be stopped in 15.7 feet after a drop of 320 feet. For all reasonable values of ρ_w (the density of the tank wall material), D of 6 inches and 20 inches, and σ_u of the order of 1000 lb_f/in^2, the second term in the denominator of Eq. (59) is negligible; also $h_e \leq h$. Thus, t_{min} determined from Eq. (58) is approximately twice t_{min} from Eq. (59) and the longitudinal stress need not be considered further.

Rearranging Eq. (56),

$$t = \frac{1.505\ R}{Y(b/D)(a_2/g_e)}\left[0.727\ R\rho\frac{g_e}{g_o} + p_o\right] \qquad (56b)$$

For any tank material, test fluid, and test acceleration, Eq. (56b) may be solved for t in terms of p_o. The value of t thus obtained may be compared with the value of t from Eq. (58) to determine whether the tank wall would be overstressed. These calculations were made and the results plotted on Fig. 6.

Assumptions were:

(1) $\overline{FS} = 2$

(2) $a_2/g_e = 10^{-4}$

(3) the test liquid is water

(4) $a_s/g_e = 20$

From Fig. 6, it is seen that for glass tanks and reasonable positive ullage pressures ($0 \leq p_o \leq 100$ psig) no tank can be constructed to produce the desired values of b/D for the drop tower test conditions. Polyethylene is a better material in this application; a 20 inch diameter test container can be designed to achieve the desired values of b/D for ullage pressures between 2.2 and 100 psig. Unfortunately, b/D = 72.5 cannot be produced with a 6 inch diameter polyethylene

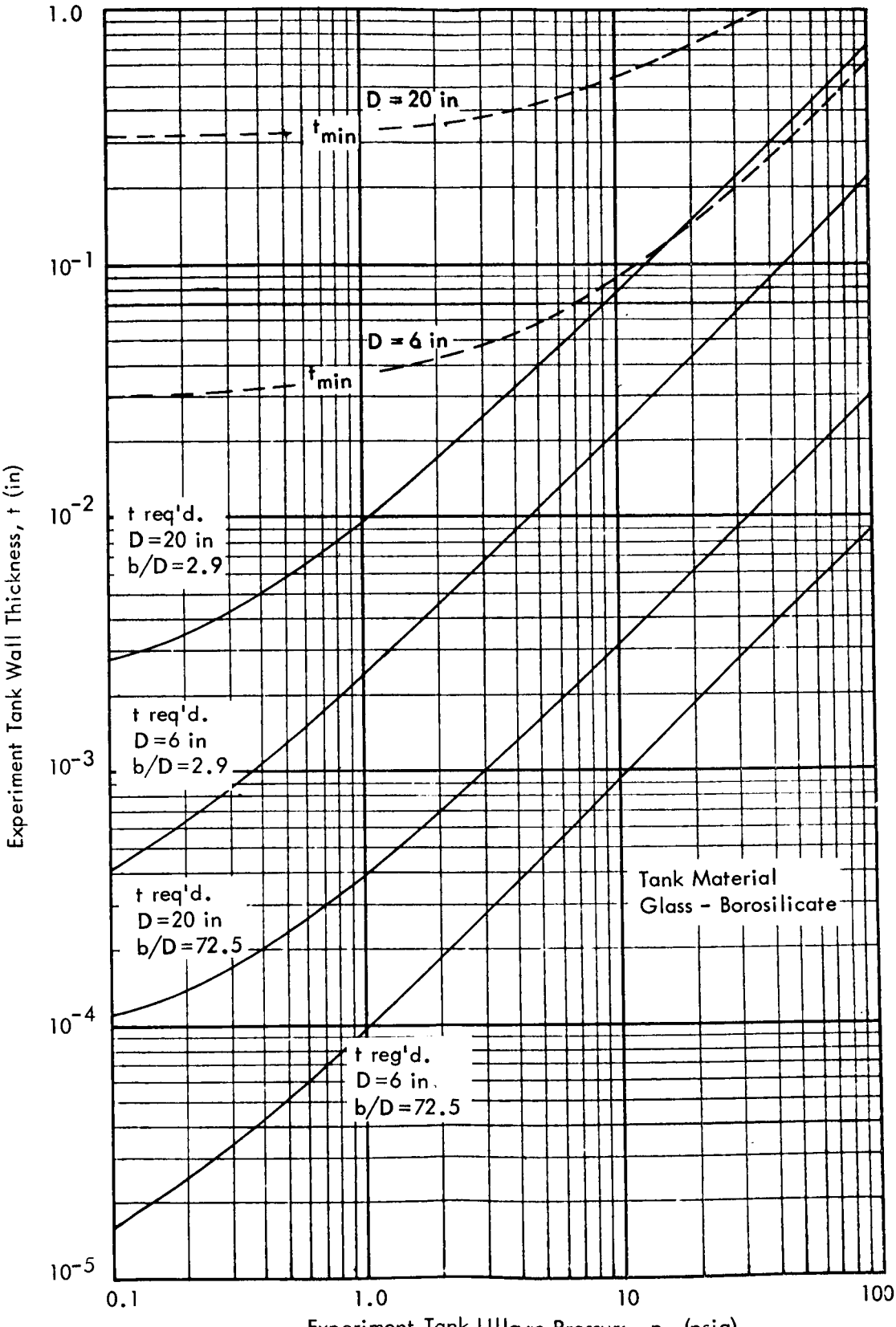

Figure 6a Experiment Tank Wall Thickness vs. Ullage Pressure

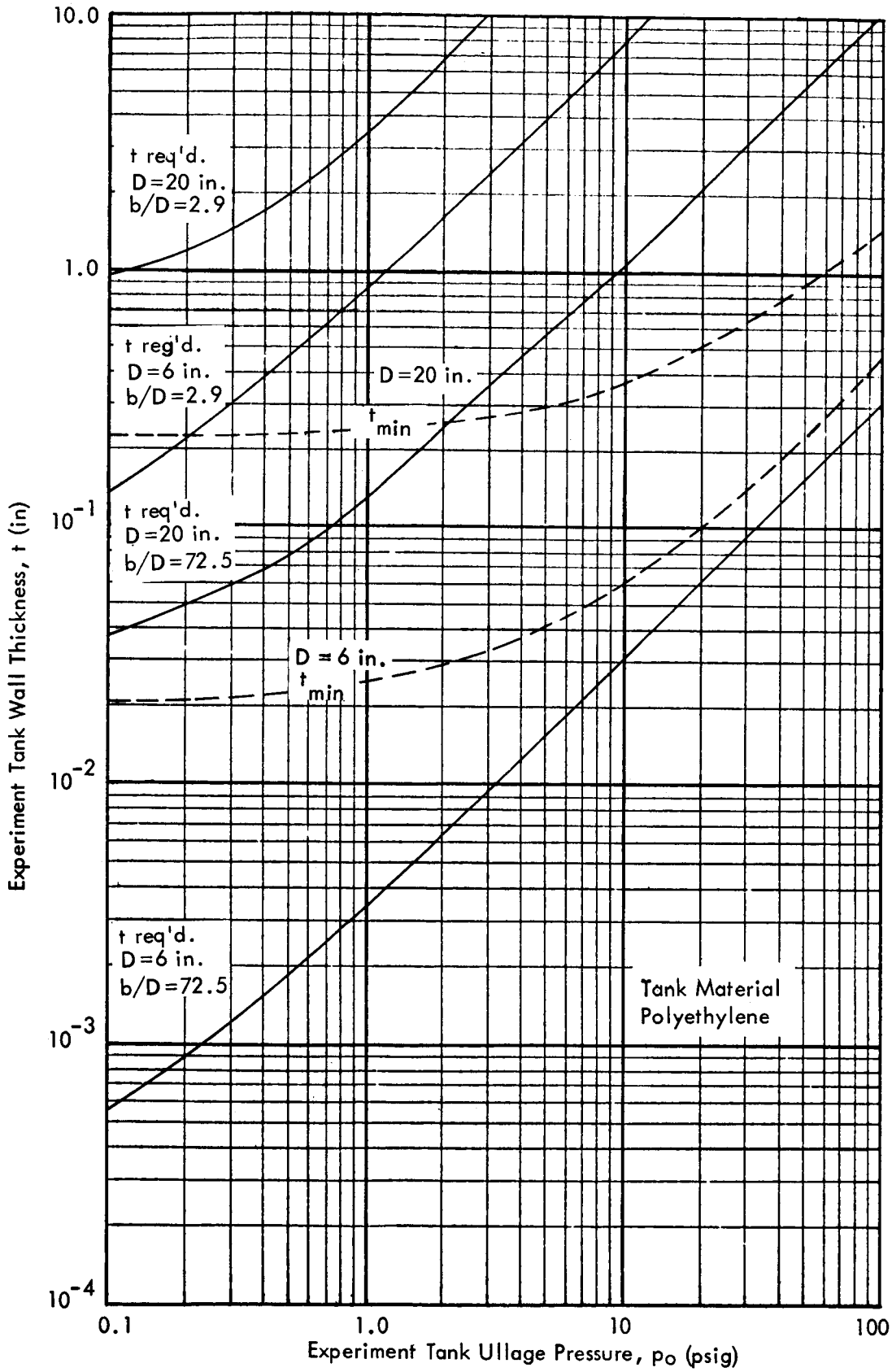

Figure 6b Experiment Tank Wall Thickness vs. Ullage Pressure

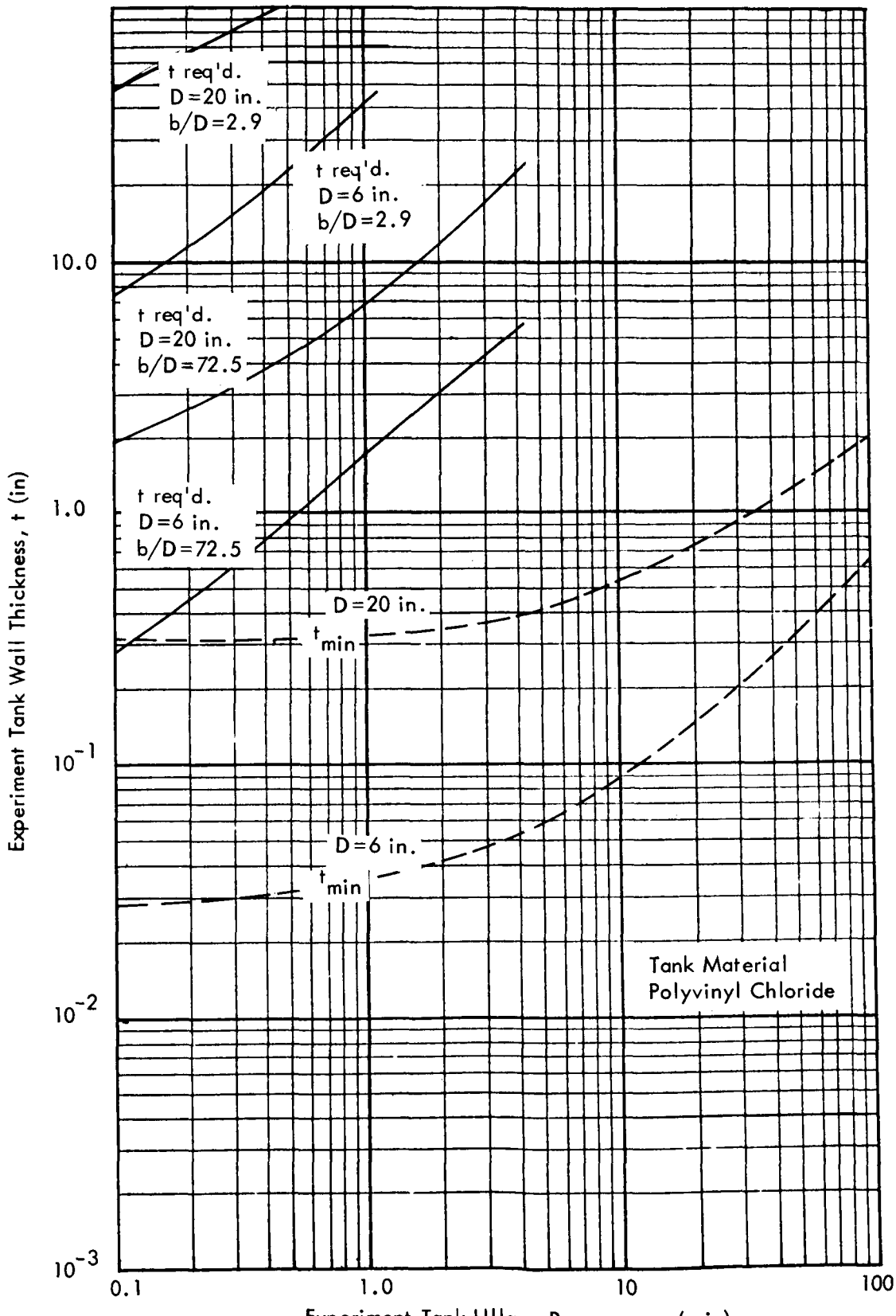

Figure 6c Experiment Tank Wall Thickness vs. Ullage Pressure

tank for $0 \leq p_o \leq 100$ psig. Polyvinyl chloride may be used over a range of ullage pressures. Thus, tanks can be constructed to simulate all desired values of b/D

To determine the means of obtaining the maximum simulated time, it is instructive to combine Eqs. (57), (45), and (43):

$$\tau_p = \frac{\tau_m}{V_p} \frac{D_p}{\sqrt{D_m}} \sqrt{2a_2 \left(\frac{b}{D}\right)}$$

Thus, for a fixed model diameter and b/D, it is desirable to make a_2 as large as possible. It is seen from Eq. (56) that this can be accomplished by making t small and p_o as large as possible for any given tank diameter and material. This condition exists where the curves of minimum and required tank wall thickness of Fig. 6 intersect. The condition of b/D = 72.5 requires a thinner tank wall with any given diameter container than does b/D = 2.9. Thus, a 20 inch diameter model tank of polyethylene and a 6 inch tank of polyvinly chloride are selected. For these containers, Eqs. (26), (46), (56), and Fig. 6 yield the data of the following table.

TABLE VI

EXPERIMENT DATA - EFFECT OF TANK WALL STORED STRAIN ENERGY

Model Tank Material	Poly.Chloride		Polyethylene	
Tank Diameter, D (in)	6	6	20	20
Simulated Prototype Acceleration (a_2/g_e)	5×10^{-4}	2×10^{-5}	5×10^{-4}	2×10^{-5}
b/D (=$E w_{go}/m a_2 D$)	2.9	72.5	2.9	72.5
Required Experiment Acceleration (a_2/g_e)	2.5×10^{-3}	10^{-4}	2.5×10^{-3}	10^{-4}
Simulated Prototype time, τ_p (sec)	148	148	81.3	81.3
We_R	0.686	0.686	7.65	7.65
Bo_R	1.906	0.076	21.2	0.848
Model Tank Wall Thickness, t (in)	0.123	0.123	0.26	0.26
Model Tank Ullage Pressure, p_o (psig)	0	0	2.2	2.2

From Table VI, it is not clear whether it is possible to make model drop tower tests for the investigation of this phenomenon. It is doubtful that the liquid surface would break, because the Weber numbers for both tank sizes considered are within the "transition" range (Fig. 1). Experiments might possibly prove that no difficulty exists with the regime of the Weber number. The Bond numbers are quite small in the case where $b/D = 72.5$. This is unimportant, however, if We and b/D are large enough to place the experiment within the inertia dominated regime. The phenomenon shares with the other phenomena the problem of insufficient test duration. The period of stage flight at $a/ge = 5 \times 10^{-4}$ can be simulated, but only the initial transients of the long coast at $a/ge = 2 \times 10^{-5}$ can be observed. If the baffles placed within the tank for reduction of sloshing are effective against this fluid motion, it may be possible to observe enough of the transient to predict damping time.

The energy stored in the liquid within the tank due to compression by the hydrostatic head is given by Eq. (24):

$$E_L = \frac{\pi R^2 \beta \rho h_e^2 (a_2 - a_1)}{2 g_o} \left[p + \frac{(a_2 + a_1)\, \rho h_e}{3 g_o} \right]$$

To reduce this equation to a form that can be examined more easily, a_2 will be eliminated because it is small relative to a_1. As in the case of the energy stored in the tank wall, the time of transition from high to low acceleration is believed critical, thus only the drop tower is considered and $a_1 = 1$ ge. The equivalent liquid depth was given as $0.79D$. Substituting:

$$E_L = 0.245\, D^4 \beta \rho \frac{a_1}{g_o} [p + 0.264\, \rho D]$$

The second term in the bracket is eliminated because it is small in comparison to the first, since for the experiment, the ullage pressure would be a minimum of 14.7 psia, the maximum value of D is 1.67 ft and a liquid density even as great as that of mercury would make the second term less than 1/5 as large as the first. Neglecting the second term:

$$E_L = 0.245\, D^4 \beta \rho \frac{a_1}{g_o} p$$

Substituting the above equation and Eq. (55) into Eq. (44)

$$b/D = 0.396\,\beta p\,\frac{a_1}{a_2}$$

Since $a_1 = ge$

$$b/D = \frac{0.396\,\beta p}{a_2/ge}$$

Following are tabulated model tank ullage pressures that would have to be used to simulate the values of b/D calculated for the assumed stage. Two full-scale vehicle conditions are considered: during ullage motor burn ($a/ge = 5 \times 10^{-4}$), and during orbital coast with continuous hydrogen venting ($a/ge = 2 \times 10^{-5}$). Also, two liquids are considered for the experiment, water, which has a compressibility (β) of 2.31×10^{-8} ft^2/lb_f; and liquid hydrogen, which has a compressibility of 7.44×10^{-7} ft^2/lb_f. The acceleration during the drop is assumed to be 10^{-4} ge, because this is the minimum that can be reliably obtained in the drop tower.

Test Fluid	Water		Liquid Hydrogen	
a/ge simulated	5×10^{-4}	2×10^{-5}	5×10^{-4}	2×10^{-5}
b/D	1.57	39.3	1.57	39.3
p required (psia)	119	2982	3.72	92.7

For water and the higher value of b/D, the required model tank ullage pressure is unreasonable because the container must be transparent to permit observation of the liquid motion. Liquid hydrogen is a hazardous fluid and would be undesirable for drop tower tests. Reference 34 lists no liquid with a value of β greater than 5 times that of water (no liquid hydrogen properties are presented in Ref. 34). Thus, the choice would be whether to use ullage pressures in the range of 600 psia or to design a facility for liquid hydrogen and to develop a transparent container to withstand an internal pressure near 100 psia at liquid hydrogen temperature (-423°F is the hydrogen saturation temperature at 1 atm.). Both of these possibilities are considered unacceptable.

VII. CONCLUSIONS AND RECOMMENDATIONS FOR FURTHER INVESTIGATIONS

A. CONCLUSIONS

From the analytical investigations described in this study, the following conclusions are drawn:

1. Propellant sloshing and thermal convection induced during space vehicle boost flight, and release of tank-wall and liquid-stored strain energy at insertion into orbit, have been identified as sources of propellant motion that will present problems in orienting liquid within propellant tanks during orbital coast.

2. The only means of attenuating these propellant motions that can be suggested is to place conventional ring type slosh baffles within the tank.

3. Low gravity testing may be accomplished in airplane flights, drop towers, or rocket flights. To achieve test durations in airplanes exceeding those available in drop towers, very small (less than 6 inch diameter) test tanks must be used. Rocket vehicles are essentially unlimited in their capability for low gravity fluid mechanics testing.

4. The initial fluid motions resulting from sloshing induced during boost flight and strain energy stored in space vehicle propellant tank walls can be investigated in drop tower tests.

5. Fluid motions resulting from thermal convection and strain energy stored in the liquid propellant can not be investigated in drop tower tests.

6. A complete investigation of liquid motion in orbital coast resulting from any of the phenomena identified will require an orbital experiment.

B. RECOMMENDATIONS

1. Future low gravity fluid mechanics investigations should be concentrated in the area of fluid dynamics, since the motions identified are severe and may well persist for several hours after insertion of the space vehicle into orbit.

2. Drop tower tests should be performed to study the initial transient fluid motions resulting from sloshing generated during boost flight and release of tank wall-stored strain energy.*

3. A large scale orbital experiment is recommended as the only available means of obtaining test data on the motions identified.**

---

* A drop tower experiment is currently in progress at Marshall Space Flight Center.

** A full scale orbital experiment was flown in July, 1966. Primary objectives of both programs are investigations of problems identified in this paper.

REFERENCES

1. NASA - Marshall Space Flight Center Memorandum R-AERO-P-100-65, "Minutes of Fifth Reference Trajectory Sub-Panel Meeting," February 25, 1965.

2. Li, T., "Cryogenic Liquids in the Absence of Gravity," Advances in Cryogenic Engineering, Vol. 1, 1961, pp. 16-23.

3. Benedikt, E. T., "General Behavior of a Liquid in a Zero or Near Zero Gravity Environment," Northrop Corporation Report ASG-TM-60-9Z6, May, 1960.

4. Merte, H., Jr., and J. A. Clark, "Boiling Heat Transfer with Cryogenic Fluids at Standard, Fractional, and Near-Zero Gravity," A.S.M.E. Paper 63-HT-28, 1963.

5. Clodfelter, R. G., "Low Gravity Pool Boiling Heat Transfer," Air Force Systems Command Technical Report APL-TDR-64-19, March, 1964.

6. Otto, E. W., "Static and Dynamic Behavior of the Liquid-Vapor Interface During Weightlessness," Presented at the Conference on Propellant Tank Pressurization and Stratification, NASA-Marshall Space Flight Center, Huntsville, Alabama, January 20 and 21, 1965.

7. Chin, J. H. et al., "Theoretical and Experimental Studies of Zero-G Heat Transfer Modes," Monthly Progress Report for the Period 3 November 1963 - 1 December 1963, Lockheed Missiles and Space Company, December 4, 1963.

8. Reynolds, W. C., "Hydrodynamic Considerations for the Design of Systems for Very Low Gravity Environments," Technical Report LG-1, Stanford University, September 1, 1961.

9. Gluck, D. F. and J. P. Gille, "Fluid Mechanics of Zero-G Propellant Transfer in Spacecraft Propulsion Systems," Trans. ASME, J. Engg. for Industry, Vol. 87, Series B, No. 1, February, 1965.

10. Bowman, T. E., "Liquid Settling in Large Tanks," Paper presented at the Symposium on Fluid Mechanics and Heat Transfer under Low Gravitational Conditions," Lockheed Research Laboratories, Palo Alto, Calif., June 24 and 25, 1965.

11. Satterlee, H. M. and W. C. Reynolds, "The Dynamics of the Free Liquid Surface in Cylindrical Containers under Strong Capillary and Weak Gravity Conditions," Stanford University Technical Report LG-2, May, 1964.

12. Eulitz, W. R., "Practical Consequences of Liquid Propellant Slosh Characteristics Derived by Nomographic Methods," National Aeronautics and Space Administration, Marshall Space Flight Center Report # MTP-P&VE-P-63-7, October 22, 1963.

13. Barnett, D. D., T. W. Winstead, L. S. McReynolds, "An Investigation of LH_2 Stratification in a Large Cylindrical Tank of the Saturn Configuration," Presented at the 1964 Cryogenic Engineering Conference.

14. "RIFT Thermodynamics Scaling Law Studies," Lockheed Missiles and Space Company Report NSP-63-117, undated.

15. Seader, J. D., W. S. Miller, L. A. Kalvinskas, "Boiling Heat Transfer for Cryogenics," Rocketdyne Report R-5598, dated May 1964.

16. "Investigation of Fluid Motion in Propellant Tanks at Engine Shutdown," Martin Company, Denver, Colorado, Proposal No. p-65-39, February, 1965 (used by special permission).

17. Swalley, F. E., G. K. Platt, and L. J. Hastings, "Saturn V Low Gravity Fluid Mechanics Problems and Their Investigation by Full Scale Orbital Experiment," Paper presented at the 1965 Low Gravity Fluid Mechanics and Heat Transfer Symposium, Sunnyvale, Calif.

18. Toole, L. E., "Residual Boost Slosh Test Program," NASA-Marshall Space Flight Center Informal Note, January, 1965.

19. Jensen, W. S., and F. E. Swalley, "Ullage Pressure in the S-IVB/Saturn V Following First Burn Shutdown," NASA-Marshall Space Flight Center Memorandum R-P&VE-PTF-64-M-125, July 7, 1964.

20. Hargis, J. H., "Thermophysical Properties of Oxygen and Hydrogen," National Aeronautics and Space Administration, Marshall Space Flight Center Internal Note IN-P&VE-P-63-13, October 28, 1963.

21. "Results of the Fifth Saturn I Launch Vehicle Test Flight" (U), NASA-Marshall Space Flight Center Report MTR-SAT-FE-64-15, April, 1964, CONFIDENTIAL (Note: Referenced data are unclassified).

22. "Sloshing Analysis," Marshall Space Flight Center Memorandum R-AERO-DD-10-66, Saturn IB-SA-203, April 27, 1966.

23. Ryan, Robert S., "Baffle Requirements for S-IVB Hydrogen Tank to Eliminate Sloshing When Entering Orbit," NASA-Marshall Space Flight Center Memorandum R-AERO-DD-31-64, March, 1965.

24. Johnston, H. L., W. E. Keller, and A. S. Friedman, "The Compressibility of Normal Hydrogen from the Boiling Point to the Critical Point at Pressures up to 100 Atmospheres," J. Am. Chem. Soc., Vol. 76, pp. 1482-1486.

25. Timoshenko, S., and G. H. MacCullough, Elements of Strength of Materials, third edition, D. Van Nostrand and Company, Inc., New York, 1949.

26. Engler, Erich, Personal Communciation, July, 1965.

27. Nast, T. C. and T. D. Sheppard, "Insulation Optimization Studies for the Operational Vehicle," Lockheed Missiles and Space Company Report TSN/65, LMSC/802574, January, 1963.

28. "The Final Report for the General Dynamics/Astronautics Zero-G Program Covering the Period from May, 1960, through March, 1962," General Dynamics/Astronautics Report AY62-0031, August, 1962.

29. NASA-Marshall Space Flight Center Informal Note, "Low 'g' Fluid Mechanics and Heat Transfer Investigation Plan," NASA-Marshall Space Flight Center Informal Note, October, 1964.

30. Swalley, F. E., "Hight Altitude Drop Experiments from a Balloon," NASA-Marshall Space Flight Center Memorandum R-P&VE-PTF-64-M-177, November, 1964.

31. "Saturn V/S-IVB Stage Modifications for Propellant Control During Orbital Venting," Douglas Aircraft Company Report SM47177, April, 1965.

32. Giedt, W. H., Principles of Engineering Heat Transfer, Van Nostrand, New York, 1957.

33. "Analytical and Experimental Study of Liquid Orientation and Stratification in Standard and Reduced Gravity Fields," Lockheed Missiles and Space Company Report 2-05-64-1, July, 1964.

34. Handbook of Chemistry and Physics, 44th Edition, The Chemical Rubber Publishing Co., Cleveland, Ohio, 1961.

BIBLIOGRAPHY

1. Harbison, J., "Preliminary Investigation of Propellant Separation After Orbital Cutoff of the Saturn IB 203, S-IVB Stage," NASA-Marshall Space Flight Center Memorandum R-P&VE-SLR-65-26, March, 1965.

2. Dearing, D. L. and R. J. Steffy, "The Significance of Parameters Affecting the Heat Transfer to the Liquid Hydrogen in the Saturn S-IVB Stage for the Lunar Orbit Rendezvous Mission," Presented to International Inst. of Refrig., Grenoble, France, June, 1965.

3. Kovas, P. J., "Effects of Fuel Tank Venting in Low-g Environment," Brown Engineering Company Report 1-PT-65, January, 1965.

October 5, 1967 APPROVAL TM X-53589

SPACE VEHICLE LOW GRAVITY FLUID MECHANICS PROBLEMS AND THE FEASIBILITY OF THEIR EXPERIMENTAL INVESTIGATION

By Gordon K. Platt

The information in this report has been reviewed for security classification. Review of any information concerning Department of Defense or Atomic Energy Commission programs has been made by the MSFC Security Classification Officer. This report, in its entirety, has been determined to be unclassified.

This document has also been reviewed and approved for technical accuracy.

C. C. WOOD
Chief, Fluid Mechanics and Thermodynamics Branch

H. G. PAUL
Chief, Propulsion Division

W. R. LUCAS
Director, Propulsion And Vehicle Engineering Laboratory

DISTRIBUTION

DIR	Dr. von Braun
DEP-T	Dr. Rees
I-DIR	General O'Connor
I-DIR	Dr. Mrazek
I-V-S-II	Mr. Godfrey
I-V-S-IVB	Mr. Meyers
I-V-S-IVB	Mr. Peters
R-DIR	Mr. Weidner
R-TO-DIR	Mr. Richard
R-TO-DIR	Mr. Vreuls
R-EO-DIR	Dr. Johnson
R-AS-DIR	Mr. Williams
R-AERO-DIR	Dr. Geissler
R-AERO-D	Mr. Horn
R-AERO-DD	Mr. Ryan (3)
R-ASTR-DIR	Dr. Haeussermann
R-TEST-DIR	Mr. Heimburg
R-TEST-C	Mr. Grafton
R-TEST-CT	Mr. Perry
R-COMP-DIR	Dr. Hoelzer
R-RP-DIR	Dr. Stuhlinger
R-RP	Dr. Heller
R-P&VE-DIR	Dr. Lucas
R-P&VE-DIR	Mr. Palaoro
R-P&VE-S	Mr. Kroll
R-P&VE-M	Mr. Kingsbury
R-P&VE-V	Mr. Aberg
R-P&VE-X	Mr. Brooksbank
R-P&VE-XN	Mr. Connell
R-P&VE-P	Mr. Paul
R-P&VE-P	Mr. Isbell
R-P&VE-PT	Mr. Wood (30)
R-P&VE-PT	Mr. Platt (20)
R-P&VE-RT	Mr. Hofues
MS-H	Mr. Akens
MS-IP	Mr. Ziak
MS-IPL	Miss Robertson (8)
Chrysler Corporation Space Division	Mr. Cannizzo
Huntsville Operations	Mr. Ziemke
1312 Meridan Street North	Mr. Messner
Huntsville, Alabama	Mr. Tode
	Mr. Kavanaugh

DISTRIBUTION (Concluded)

Douglas Aircraft Company, Inc.
5301 Bolsa Ave.
Huntington Beach, Calif. 92646

Mr. R. Holmen
Mr. D. A. Smith
Mr. R. T. Neher

Douglas Aircraft Company, Inc.
Missile and Space Systems Div.
300 Ocean Park Blvd.
Santa Monica, Calif. 90405

Mr. J. D. Schweikle

Martin-Marietta Company
P. O. Box 179
Denver, Colo. 80201

Mr. J. McGrew

NASA-Lewis Research Center
21000 Brookpark Road
Cleveland, Ohio 44135

Dr. R. J. Brum
Dr. Edward Otto

Scientific and Technical Information Facility (25)
Attn: NASA Representative (S-AK/RKT)
P. O. Box 33
College Park, Maryland 20740